DEFLECTION RESPONSE CHARACTERISTICS OF A CATHODE-RAY TUBE EMPLOYING MAGNETIC DEFLECTION

A THESIS

Presented to

the Faculty of the Division of Graduate Studies

Georgia Institute of Technology

In Partial Fulfillment

of the Requirements for the Degree

Master of Science in Electrical Engineering

by

Dana Frederic Gumb

September 1950

DEFLECTION RESPONSE CHARACTERISTICS OF A CATHODE-RAY TUBE EMPLOYING MAGNETIC DEFLECTION

Approved:

Date Approved by Chairman May 16, 1951

ACKNOWLEDGMENTS

On completion of this research, I wish to express sincere appreciation to Professor M. A. Honnell, both for his suggestion of the problem and for his invaluable assistance and encouragement in the investigation. I also wish to thank M. D. Prince for many encouraging and timesaving suggestions.

TABLE OF CONTENTS

LIST OF TABLES

LIST OF FIGURES

LIST OF LABORATORY APPARATUS

Cathode-Ray Oscilloscope, DuMont Model 304 H, Serial No. 1676.

Pulse Generator, Colonial Radio Corporation Model 700-A, Serial No. 43.

Audio Oscillator, Hewlett-Packard Model 200 C.

Oscillographic Record Camera, DuMont Model 271-A, Serial No. 162.

Electronic Frequency Meter, Hewlett-Packard, Model 500 A.

Standard Laboratory Sawtooth and Square Wave Generators.

Impedance Bridge, General Radio Company, Type 650-A.

1-B Impedance Bridge, Western Electric, Serial No. 9687.

DEFLECTION RESPONSE CHARACTERISTICS OF A CATHODE-RAY TUBE EMPLOYING MAGNETIC DEFLECTION

INTRODUCTION

Magnetic deflection of cathode-ray tubes has become increasingly important in recent years, especially with the development of large tubes for television receivers, radar indicators, and radar repeaters. Considerable information can be found in the literature concerning the basic principles of magnetic deflection, but these discussions do not indicate the actual magnetic deflection response that can be expected. It is hoped that this research will point the way toward a better understanding of magnetic deflection analogous to the well-known information on electrostatic systems.

PRINCIPLE OF MAGNETIC DEFLECTION

The purpose of this research is to study the deflection response characteristics of a cathode-ray tube employing magnetic deflection. The basic principle of deflecting an electron beam by a magnetic field is discussed by many authors.[1, 2, 3] No attempt will be made here to discuss the detailed theory other than to outline it briefly and to state the equations involved in the basic principle of magnetic deflection. The basis for this discussion was adapted mainly from J. T. MacGregor-Morris and J. A. Henley.[4]

The electron beam in a magnetically-deflected cathode-ray tube is subjected to a transverse magnetic field which deflects the beam in a plane normal to the axis of the field. The following equations and notation apply to the diagram shown in Figure 1. Two assumptions are necessary to develop this analysis. First, it is assumed that the electron beam passes through a uniform transverse magnetic field over a length a cms. of its path, and second, that the physical laws may be applied to a single electron in the beam with no edge effect. If the strength of the magnetic field is taken as H gauss and the radius of

---

[1] Manfred Von Ardenne, Cathode-Ray Tubes, (London: Sir Isaac Pitman and Sons, Ltd., 1939).

[2] Donald G. Fink, Principles of Television Engineering, (New York: McGraw-Hill Book Company, Inc., 1940).

[3] G. Parr, The Cathode-Ray Tube and Its Applications, (London: Chapman and Hall, Ltd., 1941).

[4] J. T. MacGregor-Morris and J. A. Henley, Cathode-Ray Oscillography, (Pittsburgh: Instruments Publishing Company, 1936), pp. 21-23.

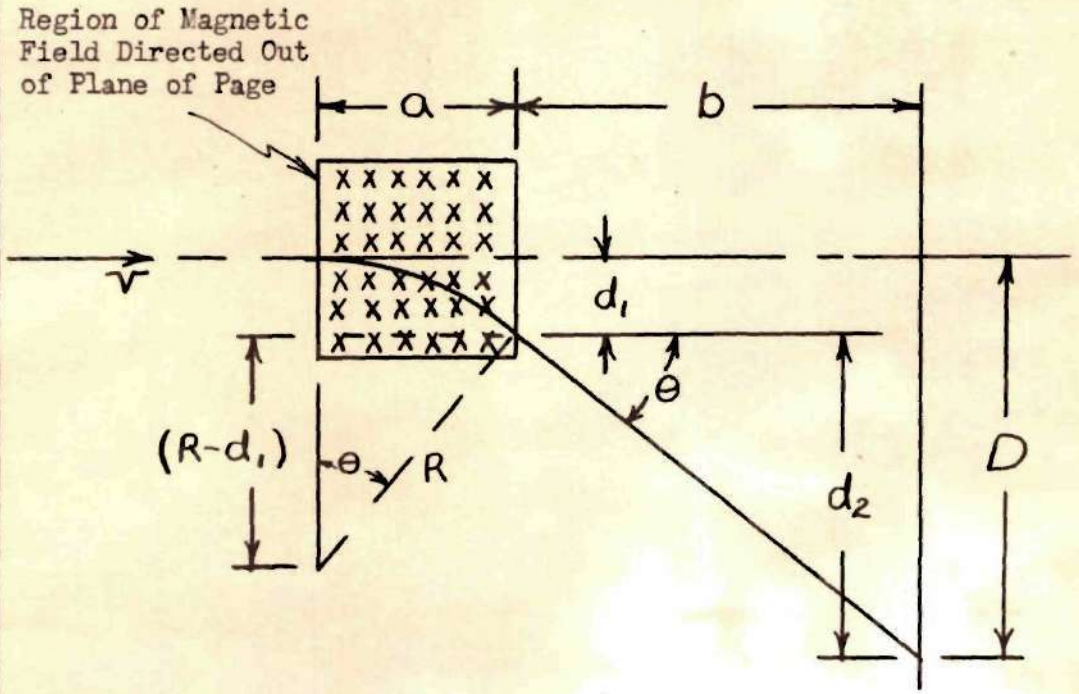

where:

v = velocity of electron beam, cms/sec.

d_1 = displacement at point of leaving magnetic field, cms.

d_2 = additional displacement obtained over length b cms.

D = total displacement from tube axis.

a = length of magnetic field assuming no fringing, cms.

b = distance from end of magnetic field to screen, cms.

R = radius of curvature of trajectory, cms.

Figure 1. Diagram Used in Analysis of Magnetic Deflection.

curvature of the trajectory of the electron beam as R cms., the equation of motion is given by

$$\frac{mv^2}{R} = Hev$$

where e = charge of electron = 4.80×10^{-10} esu

v = velocity of electron beam in cms/sec.

m = electron mass = 9.1066×10^{-28} gram.

By employing the Pythagorean theorem, the following equation in terms of R, d_1, and a is obtained:

$$(R - d_1)^2 + a^2 = R^2 .$$

If the simplifying condition is now made that θ is small, i. e., d_1^2 is negligible compared to $2Rd_1$ and that $\sin \theta \doteq \tan \theta$, the above equation reduces to

$$d_1 = \frac{a^2}{2R} = \frac{He}{2mv} a^2 \qquad \text{cms.} \qquad (1)$$

Using the above simplifying condition that $\sin \theta \doteq \tan \theta$, a relation in terms of d_2 is also obtained as

$$\tan \theta = \frac{d_2}{b} = \frac{a}{R}$$

or

$$d_2 = \frac{ab}{R} = \frac{He}{mv} ab \qquad \text{cms.} \qquad (2)$$

The total displacement from the tube axis, D, is then the sum of d_1 and d_2, i. e.,

$$D = d_1 + d_2 = \frac{He}{2mv} a^2 + \frac{He}{mv} ab \qquad \text{cms.} \qquad (3)$$

Equation (3) can be interpreted in terms of the accelerating voltage V by substituting the relation

$$v = \sqrt{\frac{2Ve}{m}} \qquad \text{cms/sec.}$$

The total deflection is then given by

$$D = H\sqrt{\frac{e}{m}} \cdot \frac{1}{\sqrt{2V}} a(b + \frac{a}{2}) \qquad \text{cms.} \qquad (4)$$

where V is the anode potential in volts.

Magnetic-deflection cathode-ray tubes have several important disadvantages. A non-uniformity of the magnetic field will cause unequal deflection of the electron beam and resultant distortion of the pattern. The phenomenon known as ion spot[5] is characteristic of magnetic deflection. The spot is a result of a beam of negative ions which are electric charges of the same charge as the electron but of considerably greater mass. This is explained by the fact that the magnetic deflection is inversely proportional to the square root of the mass of the particle as shown in Equation (4). Another serious disadvantage of magnetic deflection is the fact that the impedance of the deflecting coils varies with frequency. In this research it was desired to make a study of this last characteristic to determine the deflection response of the cathode-ray tube employing the magnetic deflection.

---

[5] Fink, op. cit., p. 139.

DESCRIPTION OF EQUIPMENT

A war surplus radar indicator was used as the basis for the development of the magnetically-deflected cathode-ray oscilloscope. The part of the indicator employed consisted of a cabinet, a 5FP7 cathode-ray tube, a focusing permanent magnet and focusing adjustment, and a deflection yoke containing two horizontal and two vertical coils with horizontal and vertical movable positioning magnets. The necessary information on the deflection coils was obtained by laboratory measurement and calculation as outlined in Appendix I.

A U. S. Army Signal Corps Type RA-105-A power supply was modified to supply the filament voltage, the - 70V grid # 1 voltage, and the + 450V grid # 2 voltage for the cathode-ray tube. A war surplus aircraft radar - 4000 volts power supply was also modified to provide the + 4000 V accelerating voltage for the indicator tube. Laboratory power supplies were used to provide the necessary filament and plate voltages required as shown on the circuit diagrams of the deflection amplifiers.

Horizontal and vertical deflection amplifiers shown in Figures 2 and 3 of Appendix III were designed and built into the oscilloscope. As can be seen from the circuit diagrams of the amplifiers, the push-pull stage of the amplifier connected to the deflection coil presents a high-impedance output so that a sawtooth wave of voltage at the input to the amplifier becomes essentially a sawtooth wave of current through the deflection coil. Adding networks are provided at the input of each phase inverter for the superposition of waveforms required to produce the three-dimensional presentations.

Laboratory variable-frequency sweep generators were used to provide the sawtooth waveforms of voltage for the deflection amplifiers. The output of each generator was differentiated to provide a pulse. One stage of an RC amplifier employing a 6SJ7 tube was built into the oscilloscope to amplify, invert, and couple this pulse to the grid of the indicator tube to blank the return trace. A Hewlett-Packard Model 200 C audio oscillator and a standard laboratory square-wave generator were used to provide the auxiliary waveforms for the three-dimensional patterns. As explained further in the section under measurements, a pulse generator, Model 700-A, Colonial Radio Corporation, was used for synchronizing purposes.

All photographs from the face of the cathode-ray tube were taken with a DuMont Type 271-A cathode-ray oscilloscope camera.

MEASUREMENTS

To obtain a measure of the deflection response of the magnetic system, standard variable-frequency sine and square waves were applied directly to one of the two vertical coils, and the response as indicated on the face of the cathode-ray tube was recorded photographically. As a note of completeness, the second vertical coil was left open-circuited during the measurements with the sine and square waves. Short-circuiting the second coil affected only very slightly the vertical amplitude.

A Hewlett-Packard audio oscillator was used to apply a variable-frequency sine wave to the deflection coil and the response was recorded photographically at frequencies of 150, 1,000, 4,000, and 10,000 cycles per second. The peak-to-peak output voltage of the generator was maintained constant at 15 volts.

Using a standard laboratory square-wave generator, photographic recordings were then made of the response at frequencies of 130, 500, 1,300 and 4,000 cycles per second. The peak-to-peak output voltage of the generator was maintained constant at 10 volts.

To produce the stationary three-dimensional patterns it was necessary to use the output of the audio oscillator as the base frequency and to synchronize the sawtooth generators and other auxiliary waveform generators with this wave. This was achieved by using the audio oscillator as the external excitation of the Model 700-A pulse generator and then by applying the positive pulse output as the synchronizing pulse for the sawtooth and square-wave generators.

A description of the various waveforms used and how they were com-

bined to produce the perspective three-dimensional patterns is given on the following pages.

DISCUSSION OF THE RESPONSE TO STANDARD WAVEFORMS

At present, few articles can be found in the literature concerning the response of a magnetic-deflection cathode-ray tube to standard voltage waveforms nor is a commercial magnetic-deflection oscilloscope available for use in the study of magnetic deflection. The basic principles of magnetic deflection have been covered quite completely by many authors as indicated earlier, but these treatments do not indicate the actual deflection response that can be expected.

E. H. Frost-Smith[6] develops an experimental method for determining the relationship between current and time, and consequently the deflection, in a linear or air-core inductive circuit with the application of a variable-frequency square wave by making use of the equation:

$$\bar{I} = \frac{i_o}{2n}\left[\epsilon^{-n} + (n - 1)\right] \qquad (5)$$

where $\bar{I}$ = mean value of the current, i_o = the final steady-state value of the current through the inductance, $n = 1/(2fT)$, and f is the square wave frequency, and T is the time constant of the inductance.

In a nonlinear circuit, his method determines the peak current with varying frequency. A plot of peak current against $\frac{1}{2f}$ then gives the current transient arising from a suddenly applied voltage to the coil.

Kurt Schlesinger[7] has approached the problem from a strictly

---

[6] E. H. Frost-Smith, "An Experimental Method of Determining the Relationship between Current and Time in an Inductive Circuit," Journal of Scientific Instruments and of Physics in Industry, Vol. 26, No. 7, (July, 1949), pp. 241-242.

[7] Kurt Schlesinger, "Magnetic Deflection of Kinescopes," Proceedings of the IRE, Vol. 35, No. 8, (August, 1947), pp. 813-821.

television viewpoint in which he has analyzed various sweep generators, the problem of transients during the retrace time, and some basic forms of sweep distortion and their elimination. He also describes a sweep circuit of improved efficiency employing power feedback and a diode as a switching element.

In this research, however, it was desired to analyze the actual response of the deflection coil to the direct application of a voltage waveform. To this end, therefore, the problem is approached from a transient viewpoint, applying the method of the transformation calculus to the equivalent circuit of the deflection coil.

Consider first the application of a sine wave of voltage to the coil. The equivalent circuit for this case is shown in Figure 2. It has been shown earlier that the deflection is proportional to the magnetic intensity H of the coil, which in turn is directly proportional to the current flowing through the coil. Therefore, the problem now is to determine the expression for the current $i_2(t)$ through the inductance as a function of time. In the following analysis, the standard notation and the table of Laplace transformations as used by Goldman[8] is followed.

The impedance of the parallel network looking to the right of terminals 1-2 is given by

$$Z(s) = \frac{(R + sL)\frac{1}{sC}}{R + sL + \frac{1}{sC}} \qquad (6)$$

[8]Stanford Goldman, Transformation Calculus and Electrical Transients, (New York: Prentice-Hall, Inc., 1949).

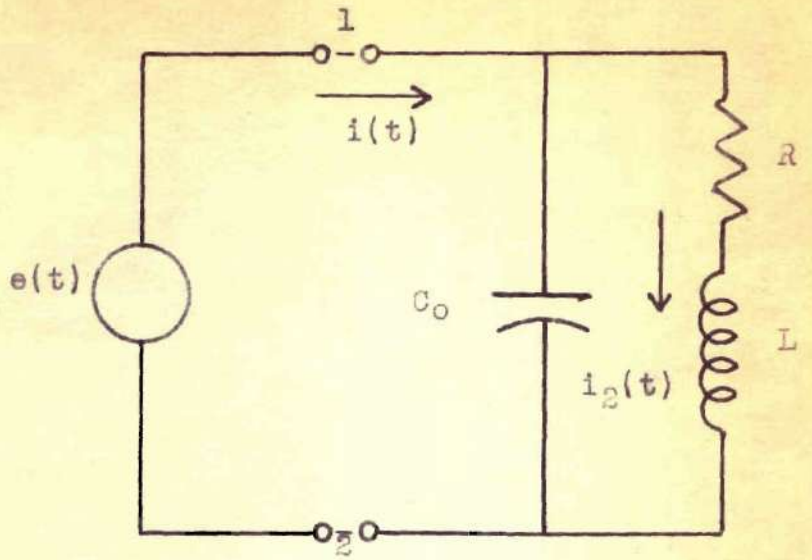

where:

e(t) = Esinwt = instantaneous applied sine wave of voltage.
i(t) = instantaneous current delivered to network.
L = inductance of deflection coil.
R = resistance of deflection coil.
C_o = distributed capacitance of deflection coil.
w = $2\pi f$.

Figure 2. Equivalent Circuit of Deflection Coil Used in Analysis of Applied Sine Wave.

Equation (6) may be written in the form

$$Z(s) = \frac{R + sL}{s^2LC + sRC + 1} \tag{7}$$

The applied voltage function in terms of s in this case is

$$E(s) = E \frac{w}{s^2 + w^2} \tag{8}$$

Therefore, the current flowing into the network as a result of the applied voltage will be

$$I(s) = \frac{E(s)}{Z(s)} \tag{9}$$

If Equations (7) and (8) are substituted in Equation (9) this becomes

$$I(s) = E \frac{w(s^2LC + sRC + 1)}{(s^2 + w^2)(sL + R)} \tag{10}$$

Now using the current division rule, the expression for the current through the inductance is found to be

$$I_2(s) = I(s) \frac{\frac{1}{sC}}{R + sL + \frac{1}{sC}} \tag{11}$$

Equation (11) may be written in the form

$$I_2(s) = I(s) \frac{1}{s^2LC + sRC + 1} \tag{12}$$

When I(s) from Equation (10) is substituted in Equation (12) this becomes

$$I_2(s) = \frac{Ew}{L} \frac{1}{(s^2 + w^2)(s + \frac{R}{L})} \tag{13}$$

Equation (13) is the final expression in terms of s for the current through the inductance. Through the use of a table of Laplace transforms,

the equation for the instantaneous current as a function of time is found to be

$$i_2(t) = \frac{Ew}{L}\left[\frac{\epsilon^{-\frac{Rt}{L}}}{(\frac{R}{L})^2 + w^2} - \frac{\cos wt}{(\frac{R}{L})^2 + w^2} + \frac{R}{wL}\,\frac{\sin wt}{(\frac{R}{L})^2 + w^2}\right] \qquad (14)$$

This equation gives the actual response that can be expected when a sine wave of voltage is applied to the deflection coil. Written in a different form, it becomes

$$i_2(t) = \frac{EwL}{R^2 + (wL)^2}\left(\epsilon^{-\frac{Rt}{L}} - \cos wt + \frac{R}{wL}\sin wt\right) \qquad (15)$$

Let us next consider a special case of Equation (15), i. e., when the resistance of the coil is zero. Although the resistance of the coil can never be zero, Equation (15) will lead to good approximations due to the fact that the resistance of the coil is, within a range of frequencies, negligible compared to the inductive reactance.

Substituting R = 0 in Equation (15) and simplifying yields the following important result:

$$i_2(t) = \frac{E}{wL}(1 - \cos wt) \qquad (16)$$

Equation (16) shows that the current function is a negative cosine wave displaced by the undying transient $\frac{E}{wL}$. This means that if the coil had no resistance, the deflection response would be the integral of the applied sine wave over all frequencies. Actually, however, the coil does have resistance which damps the transient, and the response is the negative cosine wave plus a sine term.

Consider, next, a condition where $wL \gg R$. The equation for the current becomes

$$i_2(t) \doteq \frac{E}{wL}\left(\epsilon^{-\frac{Rt}{L}} - \cos wt\right) \qquad (17)$$

where R^2 and the term $\frac{R}{(wL)^2} \sin wt$ have been neglected. The similarity between Equations (16) and (17) can be quickly noted. The $\frac{R}{L}$ factor in the exponential term is quite large in practical cases and consequently, the transient term will die out very rapidly, leaving only the minus cosine wave for the current function.

One other important fact should be noted here. The amplitude of the current, and therefore the deflection, is inversely proportional to the frequency of the applied sine wave. This is conspicuously shown in the experimental results as will be described later.

Consider now a third assumed condition where $R \gg wL$. The current equation becomes then

$$i_2(t) = \frac{EwL}{R^2}\epsilon^{-\frac{Rt}{L}} - \frac{EwL}{R^2}\cos wt + \frac{E}{R}\sin wt \qquad (18)$$

and if the $\frac{wL}{R^2}$ terms are neglected, there results

$$i_2(t) \doteq \frac{E}{R}\sin wt \qquad (19)$$

At the lower frequencies then, when the assumed condition is valid, the deflection response reproduces faithfully the applied sine function and the amplitude is limited only by the resistance of the coil.

Let us now consider some photographs of the experimental results obtained directly from the face of the cathode-ray tube. The responses obtained at four different frequencies are shown in Figures 3 through 6.

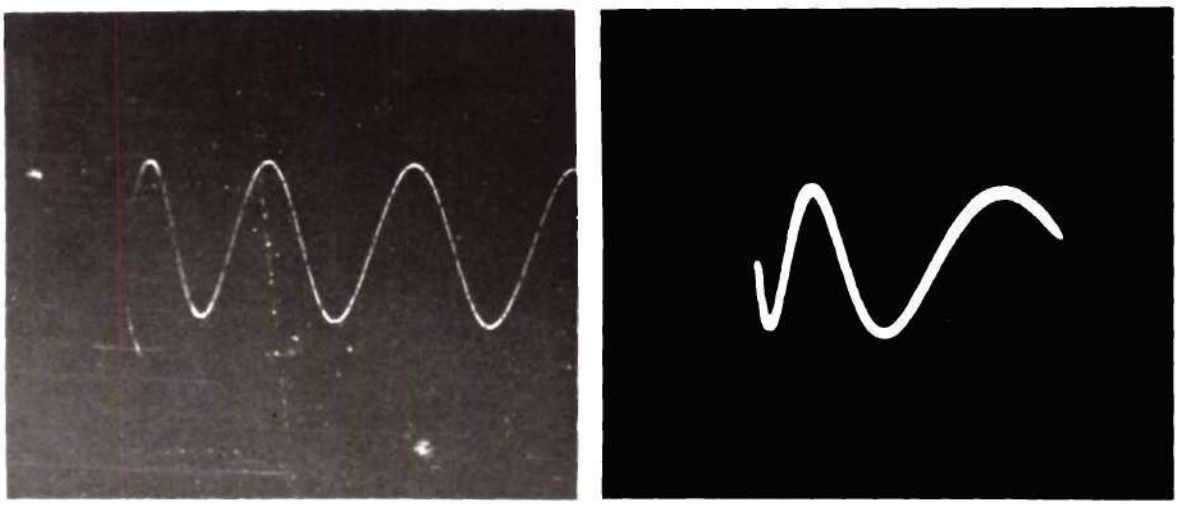

Figure 3. Input Sine Wave (left) and Deflection Response (right) at f = 150 cps.

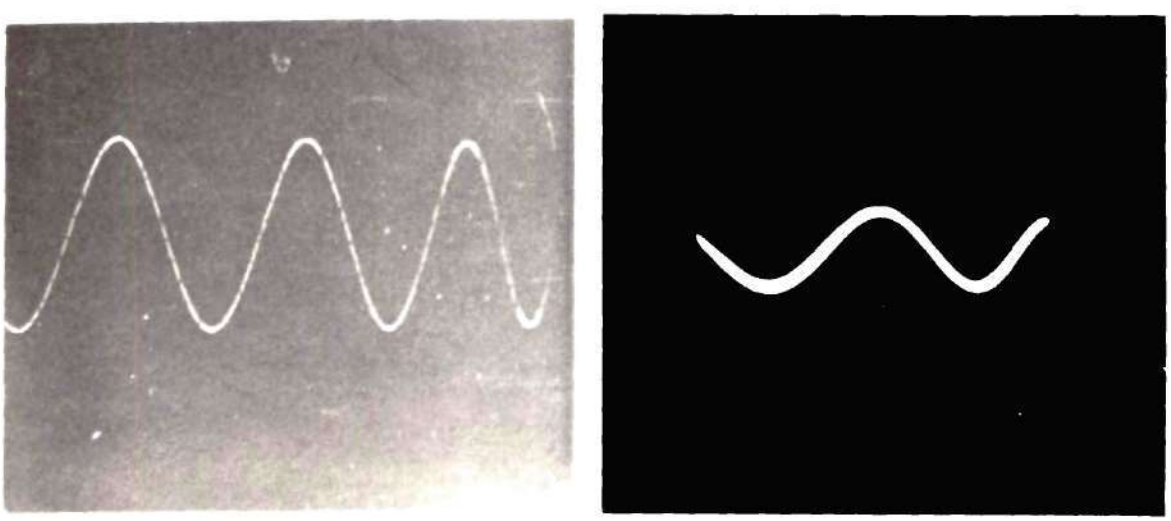

Figure 4. Input Sine Wave (left) and Deflection Response (right) at f = 1000 cps.

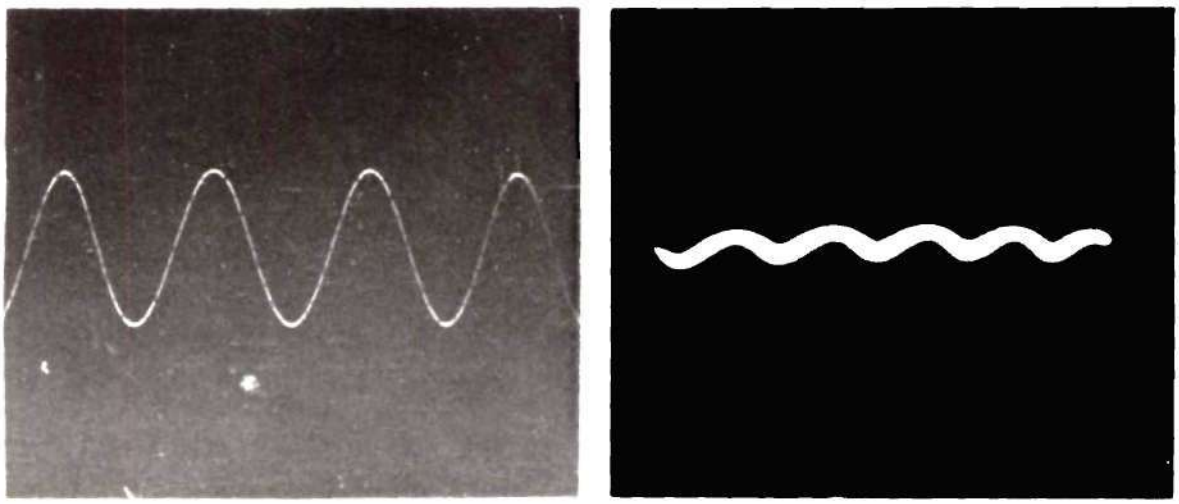

Figure 5. Input Sine Wave (left) and Deflection Response (right) at f 4000 cps.

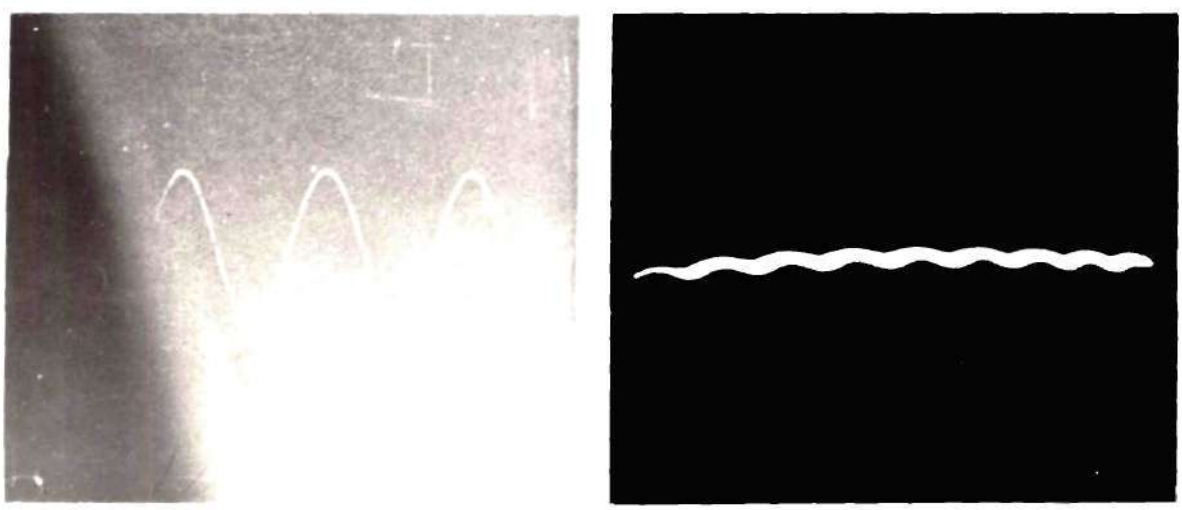

Figure 6. Input Sine Wave (left) and Deflection Response (right) at f = 10,000 cps.

For comparison, the outputs at the terminals of the generator with the deflection coil connected are shown next to the corresponding response.

Observing first the photographs taken at a frequency of 150 cycles per second, it is noted that the first cycle of the response is compressed because the horizontal deflection sweep at this frequency is nonlinear. As expected, however, the response is a sine function. In a single frequency function such as the sine wave, the two important considerations are the phase shift and the amplitude. The change in amplitude is easily recognized; but, unless a time marker were used as a reference, the phase shift between the input and the response would not be apparent. At the frequency of 150 cycles per second, the ratio of resistance to inductive reactance is approximately three to one. This approaches the assumed condition of $R \gg wL$ in the mathematical analysis, indicating that the response should be a sine function with some phase shift caused by the cosine term.

The next three photographs taken at frequencies of 1,000, 4,000, and 10,000 cycles per second respectively illustrate clearly the two important considerations mentioned with respect to the sine wave. The ratio of the inductive reactance to the resistance at 1,000 cycles per second is about 2.5 to 1, at 4,000 cycles per second about 10 to 1, and at 10,000 cycles per second about 25 to 1. All three cases are approaching the assumed condition of $wL \gg R$, indicating that the response should be a sine function approaching 90° phase shift. The photographs bear out that the response is a sine function, but the degree of phase shift is not apparent.

The second important consideration that should be noted is the

fact that the amplitude of the response decreases steadily with increasing frequency. This is shown predominantly by the photographic results. Again correlating this to the mathematics, Equation (17) shows that the current and consequently the deflection is inversely proportional to the frequency.

A square wave of voltage was chosen next to analyze for transient reproduction. The equivalent circuit of the deflection coil is as shown in Figure 2, except that for this case the applied voltage function e(t) is a square wave.

Let us consider a unit step function of amplitude k at time t = 0 and calculate the response. The voltage function in terms of t is then

$$e(t) = KU(t) \tag{20}$$

and the transformed function

$$E(s) = \frac{K}{s} \tag{21}$$

The impedance of the network is the same as in Equation (6):

$$Z(s) = \frac{R + sL}{s^2LC + sRC + 1} \tag{22}$$

and the current delivered to the network is, therefore,

$$I(s) = \frac{E(s)}{Z(s)} = \frac{K(s^2LC + sRC + 1)}{s(sL + R)} \tag{23}$$

Upon application of the current division rule, Equation (23) leads to the following solution in terms of s for the current through the inductance

$$I_2(s) = \frac{K}{L} \frac{1}{s(s + \frac{R}{L})} \tag{24}$$

and in terms of t

$$i_2(t) = \frac{K}{R}(1 - \epsilon^{-\frac{Rt}{L}}) \qquad (25)$$

A plot of this equation against time as shown in Figure 7 yields very enlightening results. The portion of the curve from t = 0 to t $= \pi\frac{L}{R}$ is the response due to the application of a unit step to the deflection coil. By superposition of a negative unit step at t $= \pi\frac{L}{R}$ the response has also been plotted for one period of a square-wave function of frequency of 427 cycles per second.

Let us consider next the application of a train of square wave pulses of amplitude E and period T as shown in Figure 8 (a). This analysis is carried out to obtain the steady-state response in closed form by means of the superposition theorem, similar to the work done by Carnahan.[9] We now need to know only the input voltage function and the indicial admittance A(t) of the deflection coil. We have determined the latter previously when the response was obtained due to the application of a step function. For convenience, the expression for the indicial admittance is repeated here:

$$A(t) = \frac{1}{R} - \frac{1}{R}\epsilon^{-\frac{Rt}{L}} \qquad (26)$$

Referring now to Figure 8 (a), we have assumed t = 0 as shown and also an infinite number of periods prior to t = 0. It is necessary then to determine the response due to the applied voltage in the period t = 0

---

[9] C. W. Carnahan, "The Steady State Response of a Network to a Periodic Driving Force of Arbitrary Shape, and Applications to Television Circuits," Proceedings of the IRE, Vol. 23, No. 11, (November, 1935), pp. 1393-1404.

Figure 7. A Graphical Plot of Equation 25 at Assumed Frequency of 427 cps.

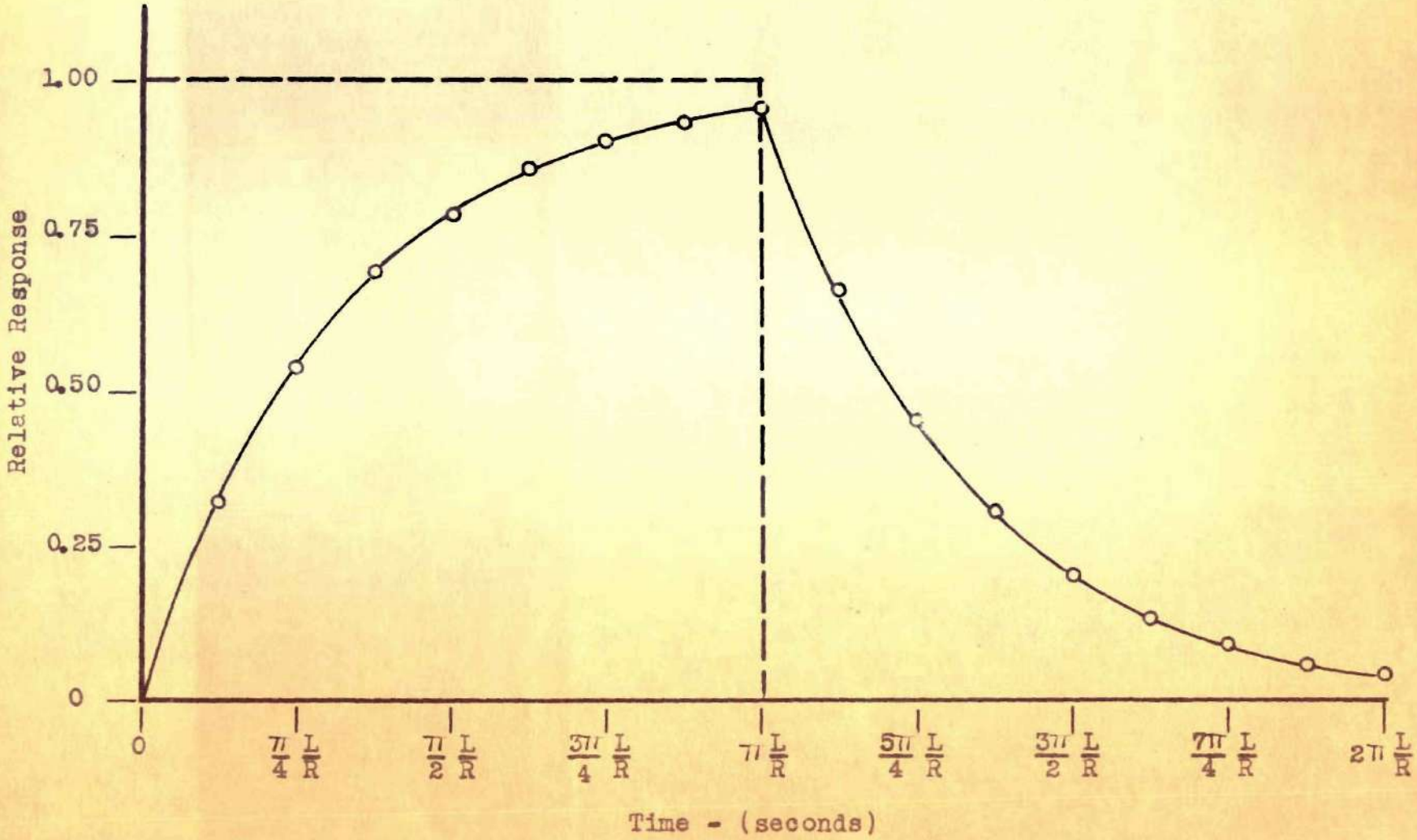

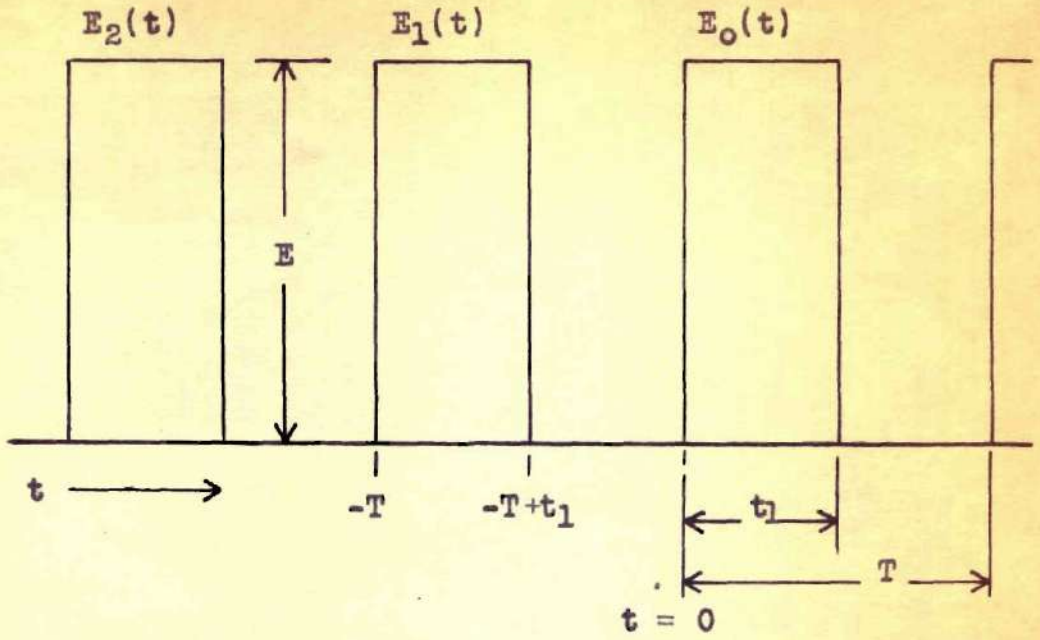

Figure 8a. Input Train of Square Wave Pulses.

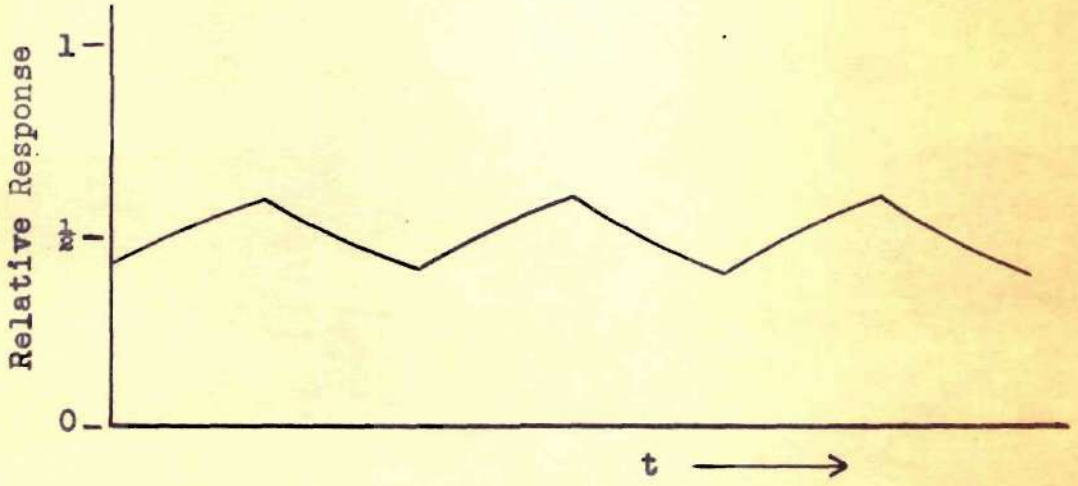

Figure 8b. Deflection Response at f = 4000 cps.

to $t = t_1$, and add to that the sum of the responses of all the preceding periods. The period $t = t_1$ to $t = T$ must be similarly considered. As stated, it is desired to use the superposition theorem to accomplish this. The superposition theorem is an expression in terms of definite integrals for the current as a function of time due to an arbitrary electromotive force, and is stated as follows:

$$i(t) = E(t_o)\, A(t) + \int_o^t A(t - \lambda) \frac{\partial E(\lambda)}{\partial \lambda}\, d\lambda \qquad (27)$$

where λ is a variable of integration. It should now be noted that the voltage function will be given as follows for the various periods:

$$\begin{aligned} E_o(t) &= E\,, \quad 0 < t < t_1 \\ E_o(t) &= 0\,, \quad t_1 < t < T \\ E_1(t) &= E\,, \quad -T < t < -T + t_1 \\ E_1(t) &= 0\,, \quad -T + t_1 < t < 0\,, \text{ etc.} \end{aligned} \qquad (28)$$

To find the response then, it is only necessary to substitute the various values of the function as given above into the superposition equation and to add the individual responses. Let us proceed step by step.

Consider the period during the pulse from $t = 0$ to $t = t_1$. Substituting first the value of $E_o(t)$ we get:

$$i(t) = E\left(\frac{1}{R} - \frac{1}{R} \epsilon^{-\frac{Rt}{L}}\right) + \int_o^t \left(\frac{1}{R} - \frac{1}{R} \epsilon^{-\frac{R}{L}(t - \lambda)}\right) \frac{\partial E(\lambda)}{\partial \lambda}\, d\lambda \qquad (29)$$

The term $\frac{\partial E(\lambda)}{\partial \lambda}$ is zero and the result is merely:

$$i(t) = E\left(\frac{1}{R}\right) + E\left(-\frac{1}{R} \epsilon^{-\frac{Rt}{L}}\right) \qquad (30)$$

This is the response due to the applied pulse at the assumed point t = 0. We must now find the response due to each of the preceding pulses. Take the first preceding pulse, for example. At the point $t = -T + t_1$ we must introduce a $-E_1(t)$ to bring the function to zero, and substituting in the superposition integral, we get

$$i(t) = -E\left(\frac{1}{R} - \frac{1}{R}\epsilon^{-\frac{R}{L}\left[t - (-T + t_1)\right]}\right) \tag{31}$$

noting again that $\frac{\partial E(\lambda)}{\partial \lambda}$ is zero. At t = - T the response is:

$$i(t) = E\left(\frac{1}{R} - \frac{1}{R}\epsilon^{-\frac{R}{L}\left[t - (-T)\right]}\right) \tag{32}$$

If we follow this same procedure for the other pulses and then take the sum, we obtain the result

$$\begin{aligned} i(t) = {} & E\left(\frac{1}{R}\right) + E\left(-\frac{1}{R}\epsilon^{-\frac{Rt}{L}}\right) - E\left(\frac{1}{R}\right) - E\left(-\frac{1}{R}\epsilon^{-\frac{R}{L}\left[t - (-T + t_1)\right]}\right) \\ & + E\left(\frac{1}{R}\right) + E\left(-\frac{1}{R}\epsilon^{-\frac{R}{L}\left[t - (-T)\right]}\right) - E\left(\frac{1}{R}\right) \\ & - E\left(-\frac{1}{R}\epsilon^{-\frac{R}{L}\left[t - (-2T + t_1)\right]}\right) + \cdots \end{aligned} \tag{33}$$

Equation (33) reduces to

$$\begin{aligned} i(t) = \frac{E}{R} - \frac{E}{R}\epsilon^{-\frac{Rt}{L}}\Big[& 1 - \epsilon^{-\frac{R}{L}(T - t_1)} + \epsilon^{-\frac{R}{L}T} - \epsilon^{-\frac{R}{L}(2T - t_1)} \\ & + \epsilon^{-\frac{R}{L}2T} \cdots \Big] \end{aligned} \tag{34}$$

or

$$i(t) = \frac{E}{R} - \frac{E}{R}\epsilon^{-\frac{Rt}{L}}\,\frac{1 - \epsilon^{-\frac{R}{L}(T - t_1)}}{1 - \epsilon^{-\frac{R}{L}T}} \tag{35}$$

Equation (35) is the expression for the steady-state response of the network during the period of the pulse.

In an entirely similar manner, the response can be determined during the time $t = t_1$ to $t = T$ when the pulse is off. It is noted that this response is the response obtained during the period of the pulse plus a negative pulse at $t = T - t_1$. In equation form, we have

$$i(t_a) = i(t) - E(\frac{1}{R}) - E(-\frac{1}{R}\epsilon^{-\frac{R}{L}(T - t_1)}) \qquad (36)$$

Substituting Equation (35) for i(t),

$$i(t_a) = \frac{E}{R} - \frac{E}{R}\epsilon^{-\frac{Rt}{L}}\frac{1 - \epsilon^{-\frac{R}{L}(T - t_1)}}{1 - \epsilon^{-\frac{R}{L}T}} - \frac{E}{R} + \frac{E}{R}\epsilon^{-\frac{R}{L}(T - t_1)} \qquad (37)$$

and simplifying, we get

$$i(t_a) = -\frac{E}{R}\epsilon^{-\frac{Rt}{L}}\frac{1 - \epsilon^{\frac{R}{L}t_1}}{1 - \epsilon^{-\frac{R}{L}T}} \qquad (38)$$

This equation is the steady-state response of the network during the periods when the pulse is off.

The graphical plot of Equations (35) and (38) presented in Figure 8(b) is very interesting. Previously in plotting the response to a unit impulse, a pulse width of $\pi\frac{L}{R}$ (or frequency of 427 cycles per second) was chosen. Data to plot Equations (35) and (38) is obtained by assuming a frequency of 4,000 cycles per second. The period T is then equal to $0.671\frac{L}{R}$. The above equations reduce to the following for this condition:

$$i(t) = \frac{E}{R} - \frac{E}{R}\epsilon^{-\frac{Rt}{L}}\frac{1 - \epsilon^{-0.335}}{1 - \epsilon^{-0.671}} \qquad (39a)$$

$$i(t_a) = -\frac{E}{R}\epsilon^{-\frac{Rt}{L}}\frac{1-\epsilon^{-0.335}}{1-\epsilon^{-0.671}} \qquad (39b)$$

and Equations (39a) and (39b) reduce to

$$i(t) = \frac{E}{R}(1 - 0.571\epsilon^{-\frac{Rt}{L}}) \qquad (40a)$$

$$i(t_a) = 0.815\frac{E}{R}\epsilon^{-\frac{Rt}{L}} \qquad (40b)$$

Table II lists the values used in plotting the above two equations. Figure 8(b) shows the complete response to the train of square waves, where $i(t)$ is plotted during the periods when the pulse is on and $i(t_a)$ during the periods when the pulse is off. The ordinate is plotted as a function of $\frac{E}{R}$.

Let us now compare the mathematical results with the experimental photographic results. The response to the application of a square wave of frequency equal to 427 cycles per second is shown in Figure 7. By referring to Figure 10, which is the experimental response at a frequency of 500 cycles per second, we can quickly see the close agreement between the theoretical and the actual results. It is noted here that at the lower frequencies, when the reactance of the coil is negligible, the response closely approximates the applied function, as shown by Figure 9. As the frequency increases, however, the reactance of the coil becomes appreciable and the applied function is integrated. This is predominantly illustrated by Figures 8(b) and 12, which are respectively the mathematical and the experimental responses to the application of a train of square waves of frequency equal to 4,000 cycles per second.

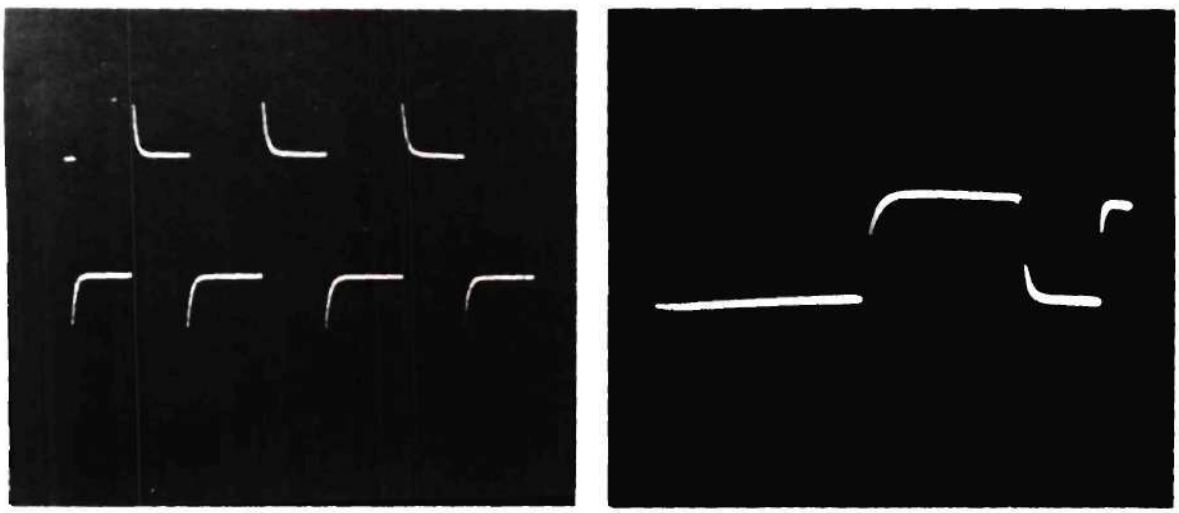

Figure 9. Input Square Wave (left) and Deflection Response (right) at f = 130 cps.

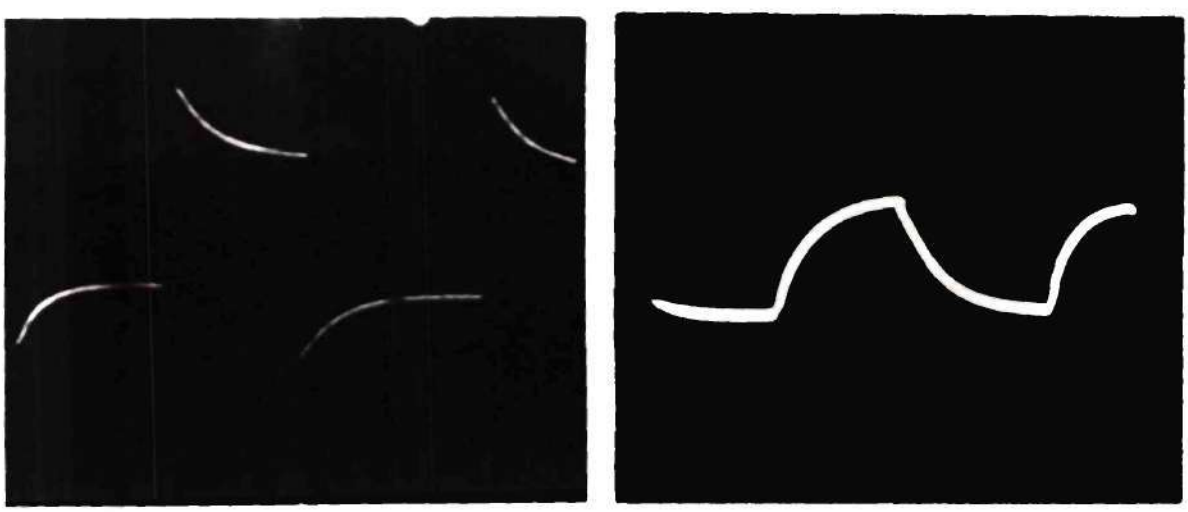

Figure 10. Input Square Wave (left) and Deflection Response (right) at f = 500 cps.

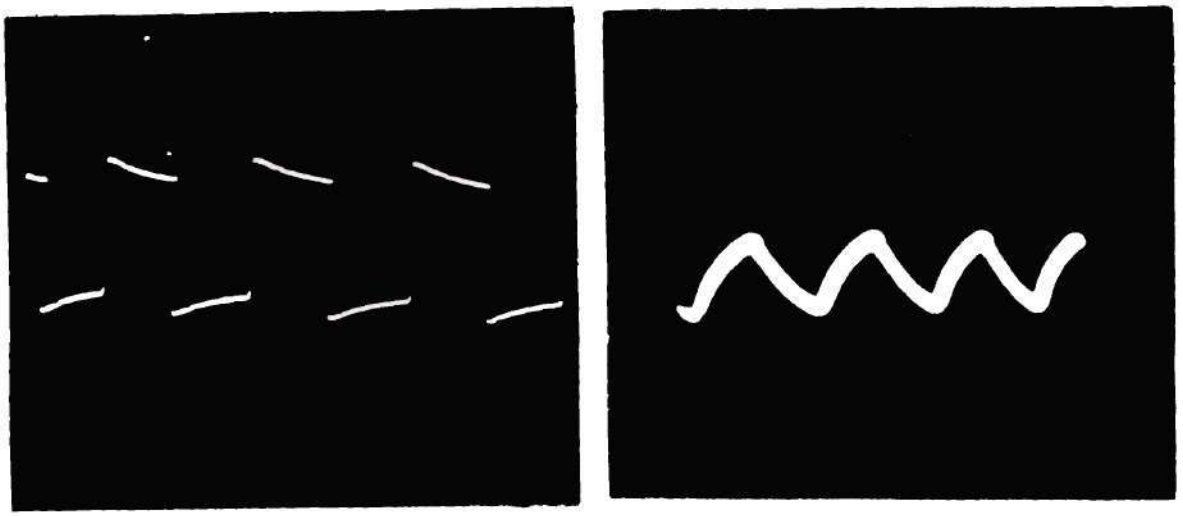

Figure 11. Input Square Wave (left) and Deflection Response (right) at f = 1300 cps.

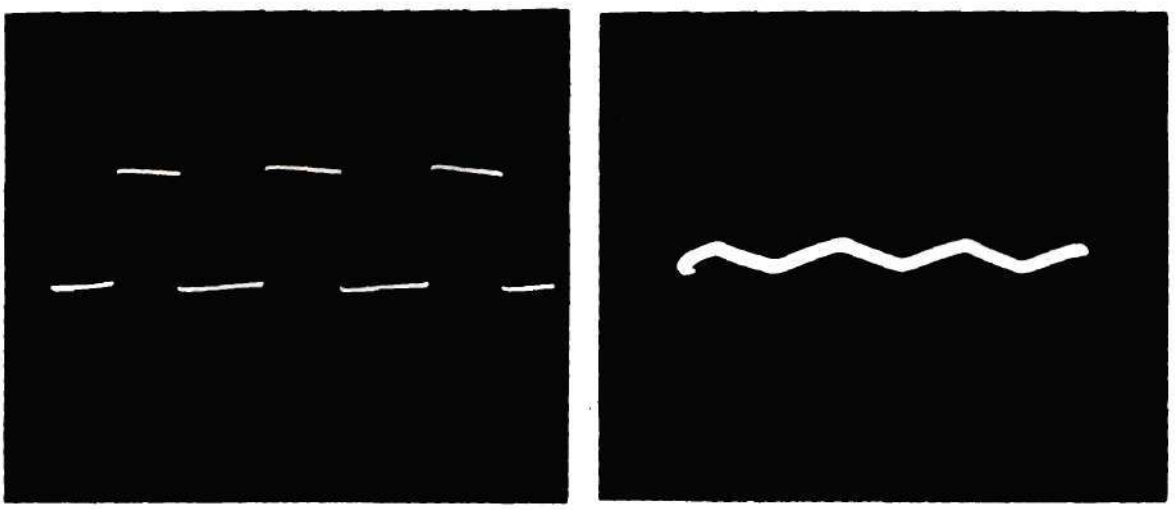

Figure 12. Input Square Wave (left) and Deflection Response (right) at f = 4000 cps.

DISCUSSION OF THE OSCILLOSCOPE PATTERNS OBTAINED WITH THE MAGNETIC-DEFLECTION OSCILLOSCOPE

To compare the magnetic-deflection oscilloscope with the standard electrostatic-deflection oscilloscope, several well-known cathode-ray oscilloscope patterns were obtained with the magnetically-deflected tube as shown in Figure 13. Both the horizontal and the vertical deflection amplifiers were used in obtaining these oscillograms. The waveforms were applied directly to the adding network at the input of each phase inverter.

The Lissajous pattern is a practical application of the oscilloscope and the response represented by the photograph with three loops in Figure 13 shows a frequency ratio of 3 to 1 between the horizontal and the vertical sine waves. The other five oscillograms in Figure 13 show varying degrees of phase shift between two sine waves each of a frequency of 180 cycles per second.

Next it was desired to set up a basic pattern similar to a television raster by applying a low-frequency sawtooth voltage to the vertical deflection amplifier and a high-frequency sawtooth voltage to the horizontal deflection amplifier. Two different cases are shown in Figure 14. Photograph (a) shows a raster built up by a vertical deflection signal of 145 cycles per second and a horizontal deflection signal of two kilocycles per second. It is observed that the vertical spacing between lines is less at the top of the raster than at the bottom. This is caused by the nonlinearity of the vertical sweep. This condition is somewhat objectionable here, but in the three-dimensional pictures it

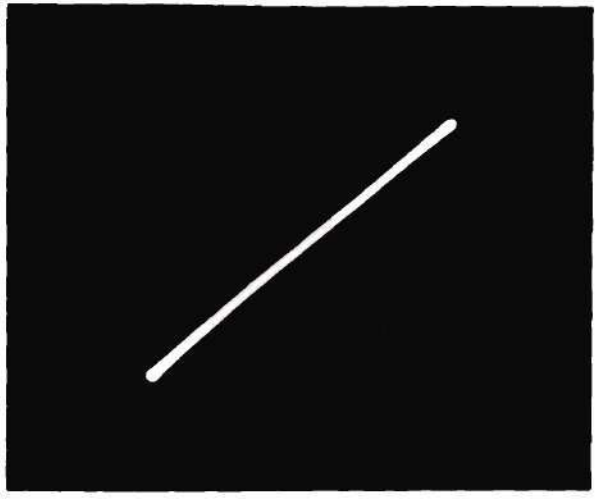

Phase Difference 0°

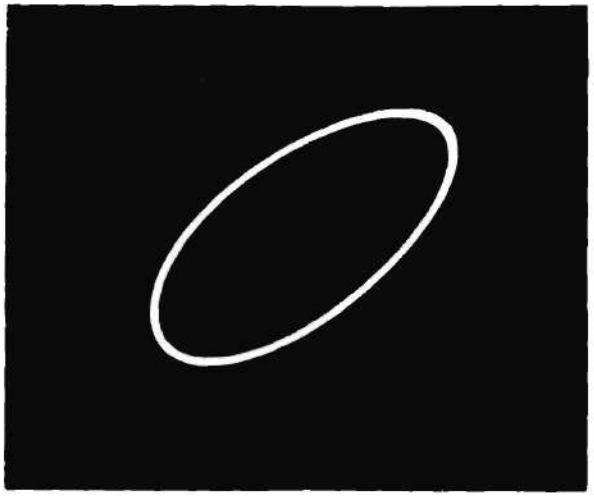

Phase Difference 45°

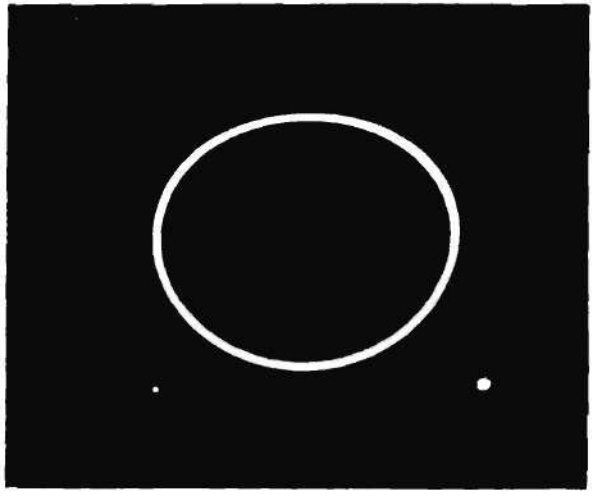

Phase Difference 90°

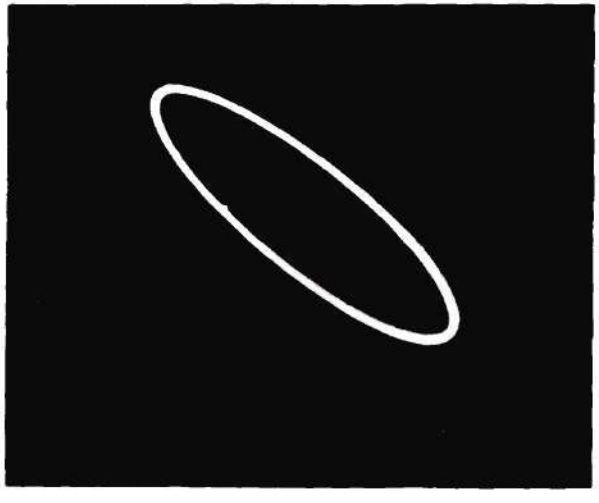

Phase Difference 135°

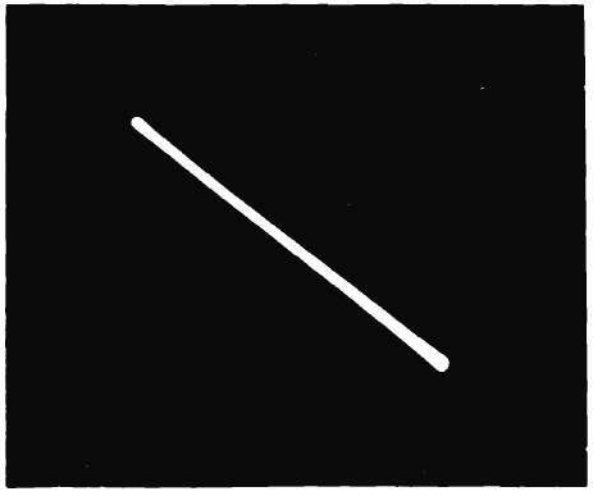

Phase Difference 180°

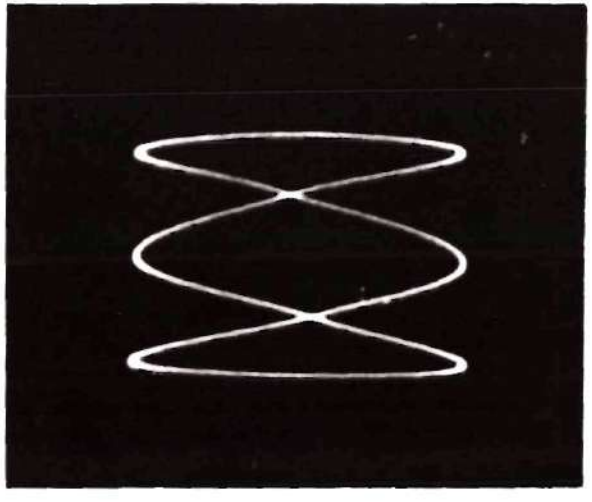

Ratio 3:1

Figure 13. Standard Oscilloscope Patterns Obtained with Magnetic Deflection

does help to give the illusion of depth. In practical applications, however, where, for instance, the depth might represent range of a radar equipment, the sweep would most likely have to be linear unless some compensation were to be made in the data which the sweep were to represent.

Photograph (b) in Figure 14 shows another raster built up this time of a vertical deflection signal of 145 cycles per second and a horizontal deflection signal of 7,800 cycles per second. The theory of the interlaced scanning in television rasters is discussed by many authors[10, 11] and will not be covered here.

Figure 16 shows very important results that were obtained by applying the principle of velocity or displacement modulation. M. A. Honnell and M. D. Prince[12] have presented a paper in which they have investigated mathematically and experimentally the velocity modulation principle in connection with a television system. The basic difference between velocity reproduction and standard television reproduction is that in the former the brightness of the spot is maintained constant and the change in brightness of the reproduced picture is achieved by varying the deflection velocity of the spot. They show how this is achieved by adding to the normal horizontal deflection voltage a portion of the video signal. A general expression is derived for the instantaneous

---

[10] Fink, op. cit.

[11] V. K. Zworykin and G. A. Morton, Television, (New York: John Wiley and Sons, 1940).

[12] M. A. Honnell and M. D. Prince, "Television Image Reproduction by Use of Velocity Modulation Principles." Paper presented at I. R. E. Convention, March, 1950.

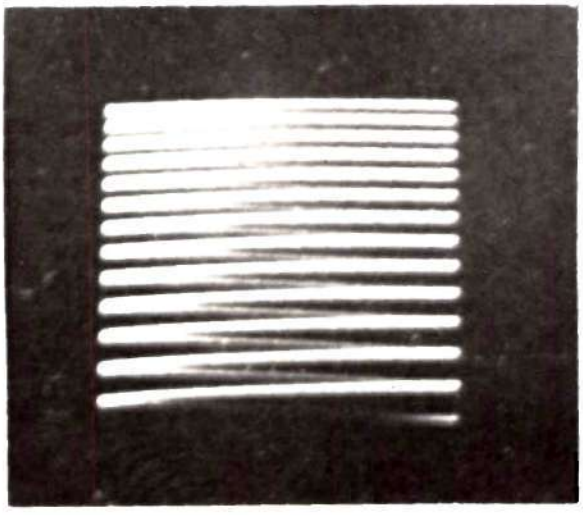

(a) H = 2 kc. sawtooth.
V = 145 cps. sawtooth.

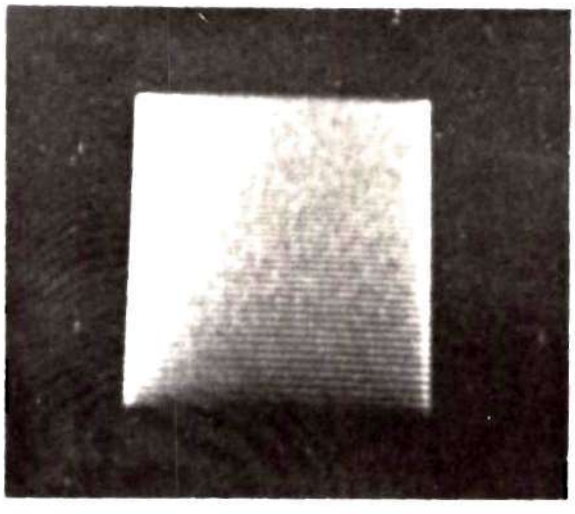

(b) H = 7.8 kc. sawtooth.
V = 145 cps. sawtooth.

Figure 14. Television Rasters.

brightness of the picture:

$$B(x) \doteq B_o \left[1 \mp Q \cdot F'(t) \right] \tag{41}$$

where

$B(x)$ = instantaneous brightness of a point at a distance x along the line;

B_o = ambient brightness of the raster;

$Q = \frac{k}{V_o}$;

V_o = unmodulated spot velocity;

$F'(t)$ = derivative of video function superimposed on horizontal deflection.

The VTR response to several types of waveforms and to printed matter is analyzed and demonstrated experimentally.

It was deemed very worthwhile to work with this same principle using the magnetically-deflected oscilloscope. The raster was built up by a vertical deflection signal of 68 cycles per second and a horizontal deflection signal of 2,200 cycles per second. A 6,000 cycles per second square wave of voltage was then added at the input of the phase inverter to the horizontal deflection amplifier. Figure 16 shows the response obtained under three different conditions which were obtained by varying the amplitude of the square wave. Condition A shows clearly the change in velocity resulting in the two vertical bright bars while Conditions B and C show two phases of an overlap condition where the spot retraces a portion of the line. In order to explain Condition A in which there is no trace overlap, reference is made to Figure 15. Part (a) of the figure shows the input square-wave voltage, part (b),

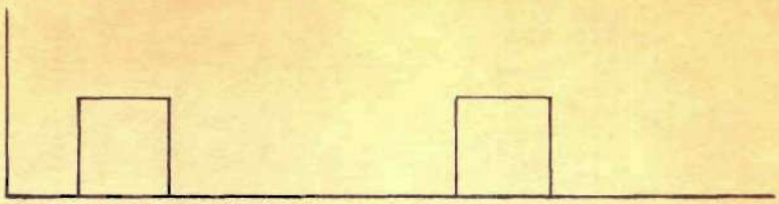

(a). Input Square Wave.

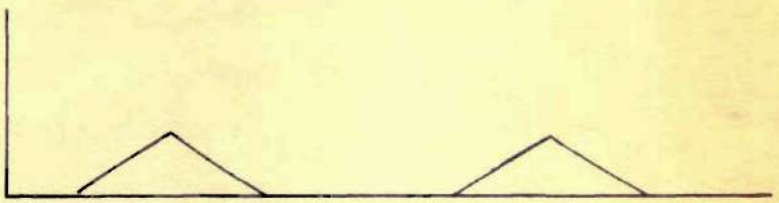

(b). Integrated Square Wave.

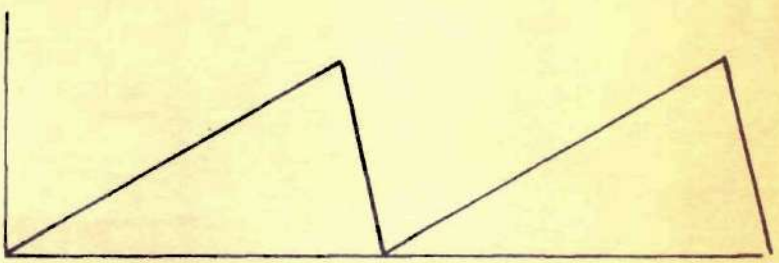

(c). Normal Deflection Function.

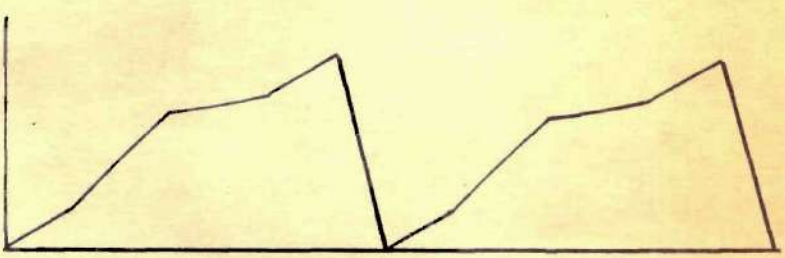

(d). Modulated Deflection Function.

Figure 15. Superposition of Modulating Function Upon Deflection Sweep.

the approximate integral of the square wave due to the fact that the current through the coil is the integral of the voltage across the coil. Part (c) shows the normal horizontal deflection signal, and part (d) the superposition of the integrated square wave upon the deflection function. It can be seen, therefore, that in one excursion the spot will experience two different velocities, the normal or unmodulated velocity and a slower or modulated velocity during that portion of the curve where the slope is greater than the normal deflection function.

Conditions B and C are obtained when the amplitude of the modulating function is such that the velocity of the spot becomes negative and a portion of the line is retraced. Condition B shows a critical point where just a little bit of retracing is noticeable and Condition C illustrates a considerable amount of retracing.

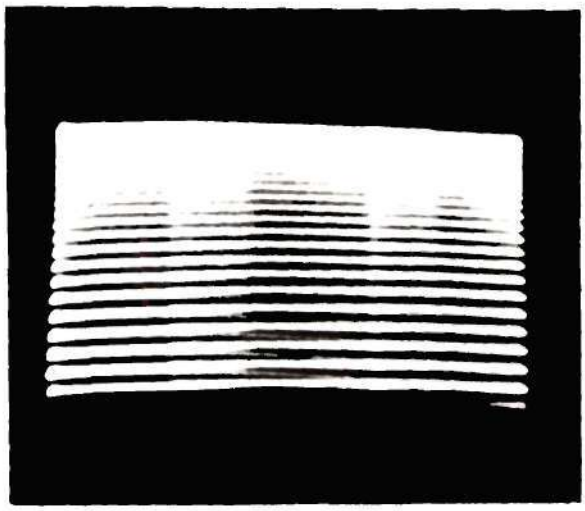

Condition A

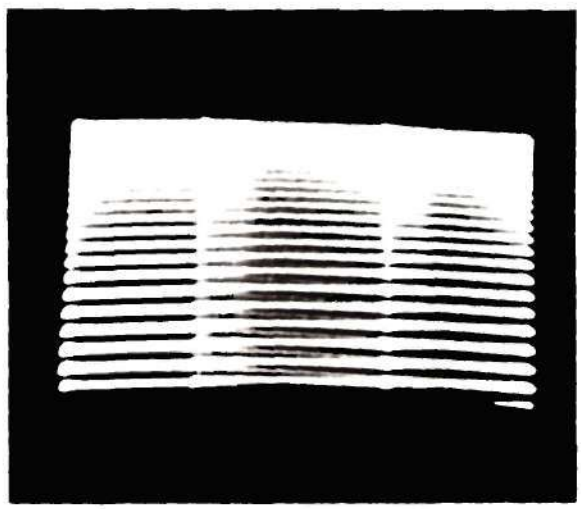

Condition B

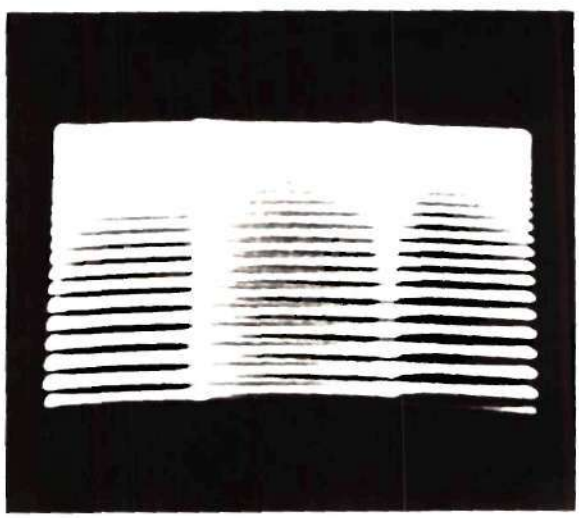

Condition C

Figure 16. Velocity Modulation

DISCUSSION OF THREE-DIMENSIONAL PRESENTATIONS

The last but probably the most interesting study that was made with the magnetically-deflected oscilloscope was that of three-dimensional presentations on the screen of the cathode-ray tube.

Otto H. Schmitt[13] has worked out mathematically the principles involved in a three-dimensional presentation in the form of isometric or other conventional projections, or as true perspective drawings. He applied the underlying principles of projective and perspective drawing and of stereoscopic photography to cathode-ray tube presentations so as to convert basic electrical data directly into vividly recognizable three-dimensional pictures.

To do this, he assumes E_x, E_y, and E_z are three supplied component voltages where x, y, and z are the cartesian coordinate axes. In a typical radar case, these components would correspond to range, elevation, and azimuth. To present an orthographic projection of the object data (E_x, E_y, E_z) on a single projection plane, he shows that there is a simple linear transformation from the three voltage components in three dimensions to the two-dimensional projection components on any specified projection plane. The direction cosines between the new and the old coordinate systems are then denoted by l_1, m_1, n_1; l_2, m_2, n_2; and l_3, m_3, n_3 respectively. The general transformation for rotation of axes then yields the three components:

---

[13]Otto H. Schmitt, "Cathode-Ray Presentation of Three-Dimensional Data," Journal of Applied Physics, Vol. 18, No. 9, (September, 1947), pp. 819-829.

$$E_{x'} = l_1 E_x + m_1 E_y + n_1 E_z \quad ,$$

$$E_{y'} = l_2 E_x + m_2 E_y + n_2 E_z \quad , \qquad (42)$$

$$E_{z'} = l_3 E_x + m_3 E_y + n_3 E_z \quad .$$

Any pair of these represents the projection on one of the coordinate planes. He explains further how these voltage components may be generated by the use of properly chosen sine-cosine potentiometers.

He investigates also what is needed to provide two suitably different sets of perspective data to be viewed by the two eyes separately to give a stereoscopic display.

Carl Berkley[14] of the DuMont Laboratories has done very enlightening experimental work in obtaining actual oblique presentations on the screen of the cathode-ray tube. In his mathematical analysis of the presentations, he derives two formulas, one for the horizontal coordinate and one for the vertical,

$$X = x - z \cos \theta \qquad (43)$$

$$Y = y - z \sin \theta \qquad (44)$$

where:

X = horizontal cathode-ray tube coordinate,

Y = vertical cathode-ray tube coordinate,

x, y, z = coordinates of point in three-dimensional space,

θ = angle the Z axis makes with the Y axis in the projection.

---

[14] Carl Berkley, "Three-Dimensional Representation on Cathode-Ray Tubes," Proceedings of the IRE, Vol. 36, No. 12, pp. 1530-1535.

By applying these formulas, he has determined the necessary X and Y functions to be applied to the horizontal and vertical deflection plates to reproduce various surfaces in perspective.

His experimental setup employed standard laboratory oscilloscopes from which he obtained his variable-frequency scanning sweeps.

Parker and Wallis[15] have done considerable work in developing three-dimensional displays directly applicable to radar presentations. They consider first truly three-dimensional displays produced by one mechanical and two electrical deflections and then, second, several perspective type displays. In analyzing these presentations the same type of mathematical analysis as employed by Schmitt[16] is used; except in the practical application, however, magslip resolver units, or selsyns, are used to obtain the necessary proportions of the inputs. Stereoscopic and polychromatic displays are also considered along with a discussion of the human factor involved in viewing such a display.

The aforementioned articles on three-dimensional presentations were found very interesting and it was desired to reproduce some of the presentations as well as to investigate other possibilities employing the magnetic-deflection oscilloscope.

As shown in the circuit diagram of the horizontal and vertical deflection amplifiers, an arrangement in the form of a "tilt switch" and "oblique control" were built into the oscilloscope so that the angle

---

[15] E. Parker and P. R. Wallis, "Three-Dimensional Cathode-Ray Tube Displays," Journal of the Institution of Electrical Engineers, Vol. 95, Part III, pp. 371-378, 1948.

[16] Schmitt, op. cit., p. 822.

at which the projection is viewed may be varied. In effect, the tilt switch connects the vertical sawtooth input through a variable potentiometer to the input of the horizontal phase inverter, the setting of the potentiometer determining the proportion that is fed to the horizontal circuit.

Following the same method as used by Berkley[17], let us next analyze mathematically some of the patterns obtained. In this analysis, we assume sawtooth waves of current represented by

$$x = nk_1t \tag{45}$$

and

$$z = k_2t \tag{46}$$

where x = a sweep in the three-dimensional x direction;

z = a sweep in the three-dimensional z direction;

n = frequency ratio between sweeps;

k_1, k_2 = amplitude constants;

t = time.

Consider first the plane $y = 0$ passing through the origin. By using Equations (43) and (44), we find that this surface can be represented by applying to the horizontal amplifier the function

$$\begin{aligned} X &= x - z \cos \theta \\ &= nk_1t - k_2t \cos \theta \end{aligned} \tag{47}$$

where $\cos \theta$ is the fraction of the z value that must be added to the x value to obtain the proper cathode-ray tube horizontal coordinate, and

---

[17] Berkley, op. cit., p. 1532.

then by applying to the vertical amplifier the function

$$Y = y - z \sin \theta$$
$$= - k_2 t \sin \theta \qquad (48)$$

where sin θ also determines the fraction of the z value that must be added to the y value to obtain the proper vertical coordinate. Equations (47) and (48) are the parametric equations for the reproduction of a plane passing through the origin. This plane is shown in Figure 17 (a).

Let us next consider the surface

$$B \sin z - x = 0 \qquad (49)$$

Using Equation (43) again, we find that the horizontal function is the algebraic sum of the high-frequency sweep and a proportion of the low-frequency sweep plus the function

$$x = B \sin z \qquad (50)$$

expressed as

$$X = nk_1 t - k_2 t \cos \theta + B \sin z \qquad (51)$$

Similarly, by employing Equation (44) for the vertical function, we get

$$Y = k_2 t \qquad (52)$$

which is the vertical low-frequency sweep alone. Equations (51) and (52) are the parametric representations of the surface in Equation (49). This surface is shown in Figure 17 (b).

Consider now the surface

$$y = A \sin z \tag{53}$$

This can be seen to be developed by applying to the horizontal amplifier the function

$$X = nk_1t - k_2t \cos \theta \tag{54}$$

and to the vertical amplifier the functions

$$y = k_2t \ , \tag{55}$$

the sweep, and

$$y = A \sin z \tag{56}$$

This surface is represented in Figure 17 (c).

Figure 17 (d) is also very interesting in that it shows a combination of the previous two examples. The vertical function remains the same, i. e., the algebraic sum of the vertical sweep and $y = A \sin z$. The horizontal function contains the algebraic sum of the high-frequency sweep and a proportion of the low-frequency sweeps plus the function $x = B \sin z$.

Many other interesting and unusual patterns were obtained on the oscilloscope by adding different functions to the basic plane. Figures 1 through 5 of Appendix IV illustrate some of the more striking projections that were photographed directly from the screen of the cathode-ray tube. Under each photograph, the functions that were combined at the input of each phase inverter to produce the pattern shown are indicated.

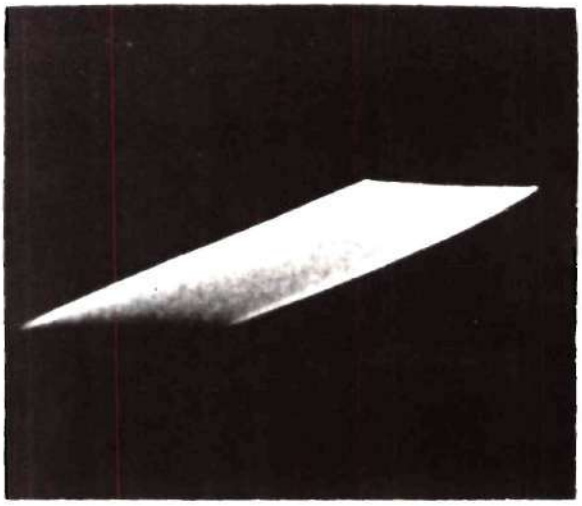

(a) Plane, y=0.
V = 145 cps. sawtooth.
H = 13 kc. sawtooth +
145 cps. sawtooth.

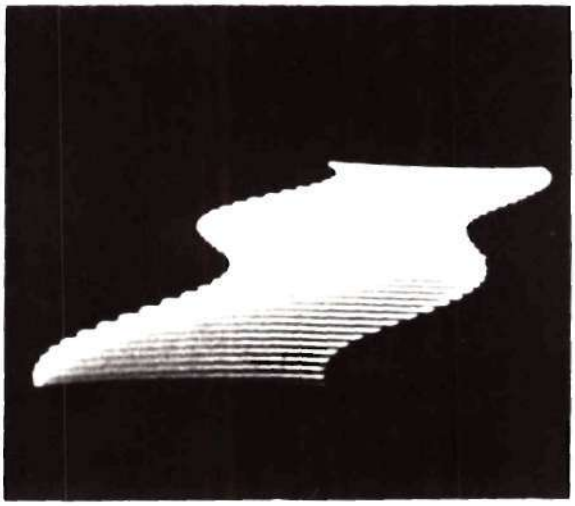

(b) Surface, Bsinz-x=0.
V = 145 cps. sawtooth.
H 6.2 kc. sawtooth +
145 cps. sawtooth +
310 cps. sine wave.

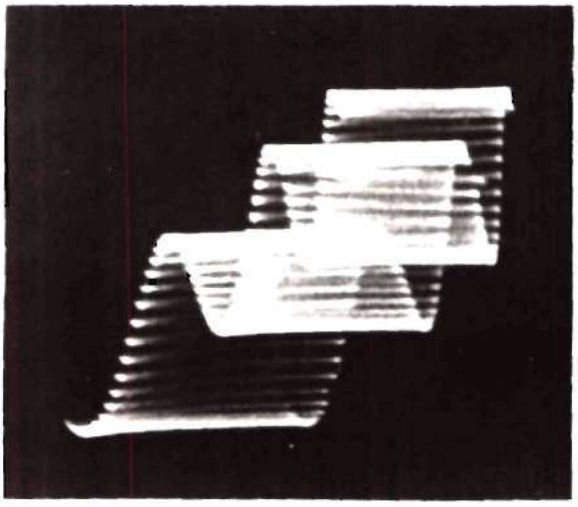

(c) Surface, Asinz-y=0.
V = 145 cps. sawtooth +
450 cps. sine wave.
H = 12.8 kc. sawtooth +
145 cps. sawtooth.

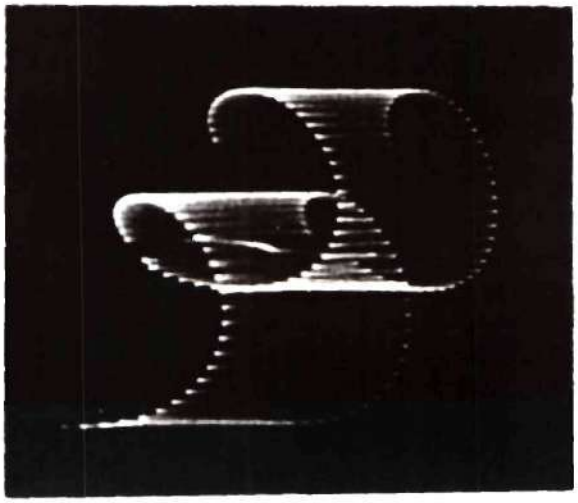

(d) Surface, Bsinz-x=0 plus
Asinz-y=0.
V = 145 cps. sawtooth +
340 cps. sine wave.
H = 13 kc. sawtooth +
145 cps. sawtooth +
315 cps.sine wave.

Figure 17. Three-Dimensional Surfaces.

CONCLUSIONS

In conclusion, there are several important facts that bear reviewing. In considering the magnetic deflection of a cathode-ray tube, it is well to remember that the voltage across the coil is equal to the product of the inductance of the coil and the time rate of change of the current through the coil. The response, therefore, would always be the integral of the applied function if the resistance of the coil were zero. Since this resistance cannot be ignored, however, the degree of integration is dependent upon the frequency, which determines the ratio of the inductive reactance to the resistance.

There are several ways by which a desired response can be obtained on the cathode-ray tube. The input voltage function can be operated on before being applied to the coil so that the integral of the applied function is the desired response. Another method is to supply the coil from a constant-current generator so that the current wave will be approximately the same as the voltage function applied to the generator. Another possibility would be to shunt an external capacitance and resistance across the coil with the proper magnitude to make the impedance of the circuit equal to $\sqrt{\frac{L}{C}}$ at all frequencies.

This investigation has shown that it is possible to duplicate the well-known traces obtained on electrostatic deflection oscilloscopes by magnetic-deflection means. It appears rather striking that no magnetic-deflection oscilloscope is available as a commercial instrument. This seems even more unusual considering the number of magnetically-deflected cathode-ray tubes that are now used in present-day television receivers and radar indicators.

BIBLIOGRAPHY

Berkley, Carl, "Three-Dimensional Representation on Cathode-Ray Tubes," Proceedings of the Institute of Radio Engineers, XII, Vol. 36, December, 1948, pp. 1530-1535.

Carnahan, C. W., "The Steady-State Response of a Network to a Periodic Driving Force of Arbitrary Shape and Applications to Television Circuits," Proceedings of the Institute of Radio Engineers, XI, Vol. 23, November, 1935, pp. 1393-1404.

Clarke, James G., "Differentiating and Integrating Circuits," Electronics, No. 11, Vol. 17, November, 1944, pp. 138-142.

Fink, Donald G., Principles of Television Engineering, New York and London: McGraw-Hill Book Company, Inc., 1940, 541 pp.

Frost-Smith, E. H., "An Experimental Method of Determining the Relationship between Current and Time in an Inductive Circuit," Journal of Scientific Instruments and of Physics in Industry, No. 7, Vol. 26, July, 1949, pp. 241-242.

Massachusetts Institute of Technology Radar School Staff, Principles of Radar, New York: McGraw-Hill Book Company, 1948, 746 pp.

Parker, E. and P. R. Wallis, "Three-Dimensional Cathode-Ray Tube Displays," Journal of the Institution of Electrical Engineers, III, 37, Vol. 95, September, 1948, pp. 371-87.

Parr, G., The Cathode-Ray Tube and Its Applications, London: Chapman and Hall, Ltd., 1941, 180 pp.

Rawcliffe, D. and R. W. Dressel, "Magnetic Focusing and Deflection," Electronic Industries, October, 1946, pp. 52-56.

Schade, Otto H., "Magnetic Deflection Circuits for Cathode-Ray Tubes," RCA Review, No. 3, Vol. VIII, September, 1947, pp. 506-538.

Schlesinger, Kurt, "Magnetic Deflection of Kinescopes," Proceedings of the Institute of Radio Engineers, VIII, Vol. 35, August, 1947, pp. 813-821.

Schmitt, O. H., "Cathode-Ray Presentation of Three-Dimensional Data," Journal of Applied Physics, No. 9, Vol. 18, September, 1947, pp. 819-829.

Von Ardenne, Manfred, Cathode-Ray Tubes, London: Sir Isaac Pitman and Sons, Ltd., 1939, 530 pp.

Zworykin, V. K. and G. A. Morton, Television, New York: John Wiley and Sons, 1940, 646 pp.

APPENDIX I

MEASUREMENTS MADE ON DEFLECTION COILS

MEASUREMENTS MADE ON DEFLECTION COILS

When work was first started on the magnetic-deflection oscilloscope, no information pertaining to the characteristics of the deflection coils was available. It was desired to have some information on the coils; therefore, several simple laboratory measurements were made as described below.

First, it was desired to determine the inductance and the distributed capacitance of the coils. It should be noted here that the complete deflection yoke consisted of four independent coils, each with its own external connection points. Two of the four coils were for vertical deflection and the other two for horizontal deflection. The two coils in each case were found to be identical pairs. Complete measurements, therefore, were made only on one of the two for the vertical and for the horizontal.

To obtain data a circuit such as shown in Figure 1 was set up. The precision condenser C was set at various values as shown in the tabulated data and then the input sine wave varied in frequency to obtain a resonant point. In making computations, the input capacitance of the vacuum tube voltmeter probe of 6 uuf and the 10 uuf capacitance of the leads to the precision condenser were subtracted from C to obtain a new value C'.

The theory involved in determining the inductance and the distributed capacitance is based upon the equation for the resonant frequency of the circuit:

$$f^2 = \frac{1}{4\pi^2 L(C + C_o)} \qquad (1)$$

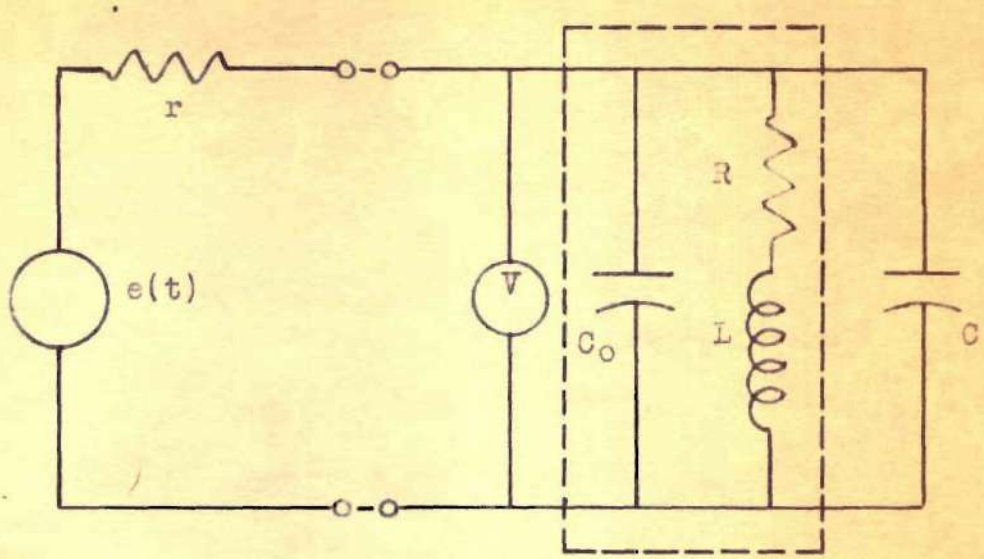

where:

e(t) = variable frequency sine wave.
r = 10,000 ohms.
V = vacuum tube voltmeter with probe.
L = Inductance of coil.
R = Resistance of coil.
C_o = Distributed capacitance of coil.
C = Shunting precision capacitance.

Figure 1. Circuit Diagram for Determining Parameters of Deflection Coils.

where

f = frequency of applied sine wave,

L = inductance of coil,

C_o = distributed capacitance of coil,

C = shunting capacitance.

Rearranging Equation (1) we obtain:

$$\frac{1}{f^2} = 4\pi^2 LC + 4\pi^2 LC_o \qquad (2)$$

which is of the form:

$$y = mx + b \qquad (3)$$

It can be seen, therefore, that a plot of $\frac{1}{f^2}$ versus C' will enable a determination of the inductance and the distributed capacitance. The data taken for the horizontal and vertical coils are plotted in Figure 2. The slope of the line is equal to $4\pi^2 L$ and the x intercept is the distributed capacitance.

Sample computations for the two coils are as follows:

Vertical Coil:

a. Slope $= 4\pi^2 L = \frac{(4.0 - 1.9) \times 10^{-9}}{(400 - 100) \times 10^{-12}} = 7$

Therefore $L = 177.8$ mh

b. From the curve:

$$C_o = 168 \text{ uuf}$$

Horizontal Coil:

a. Slope $= 4\pi^2 L = \frac{(0.93 - 0.35) \times 10^{-9}}{(400 - 100) \times 10^{-12}} = 1.932$

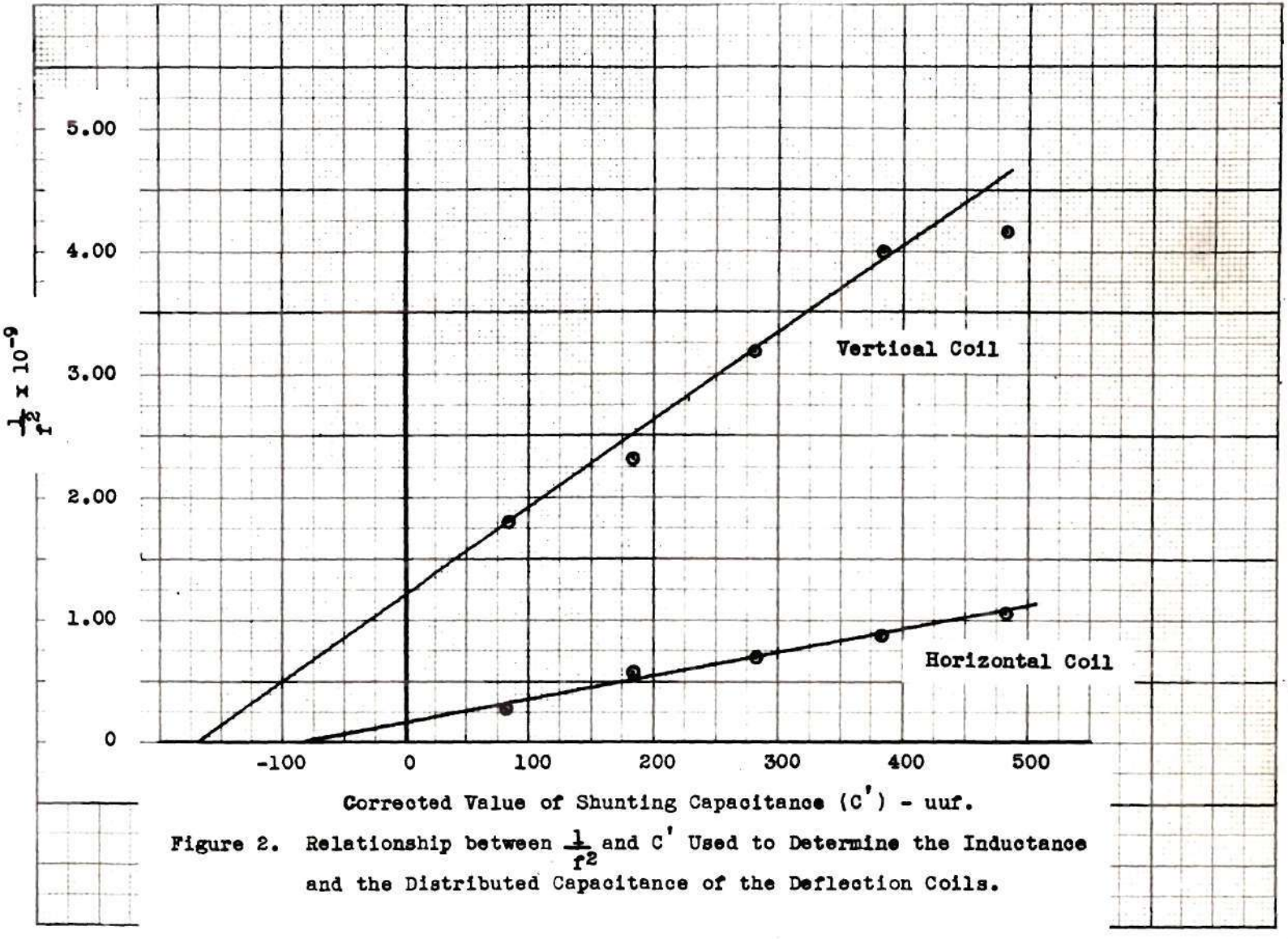

Figure 2. Relationship between $\frac{1}{f^2}$ and C' Used to Determine the Inductance and the Distributed Capacitance of the Deflection Coils.

Therefore $L = 48.9$ mh

b. From the curve:

$$C_o = 88 \text{ uuf}$$

Second, it was desired to determine the effective resistance of the coil. Measurements were made using two different impedance bridges. First, the laboratory General Radio Company Impedance Bridge, Type 650-A, was used to measure the inductance and the Q of the coil at a frequency of 1000 cycles per second. The effective resistance was then computed as shown below in the sample computations.

Horizontal Coil:

Measured: $L = 43$ mh

$Q = 1.1$

$f = 1000$ cycles per second

Calculated: $R_{a-c} = \frac{wL}{Q} = 246$ ohms.

Vertical Coil:

Measured: $L = 182$ mh

$Q = 2.4$

$f = 1000$ cycles per second

Calculated: $R_{a-c} = \frac{wL}{Q} = 476$ ohms.

As a check, the second bridge employed was the laboratory Western Electric 1-B Impedance Bridge, Serial No. 9687. Readings were taken this

time at a frequency of 200 cycles per second. The data obtained is tabulated below.

Horizontal Coil:

$L = 41$ mh

$R = 244$ ohms

Vertical Coil:

$L = 185$ mh

$R = 477$ ohms

Third, the d-c resistance of the coils was measured using a standard ohmmeter and a laboratory decade resistance. The values are:

Horizontal Coil: $R_{d-c} = 240$ ohms

Vertical Coil: $R_{d-c} = 480$ ohms

Fourth and last, measurements were made to determine the deflection current required for full scale deflection of the spot. Consider first the horizontal coils. Using one of the pair of coils required 130 ma to deflect the spot from the center of the tube to one side. Using the two coils in series aiding, however, required only 70 ma. With the vertical coils, 90 ma was required to deflect from center to top using one of the pair of coils, and 45 ma using the two coils in series aiding.

APPENDIX II

TABLES

TABLE I

Calculated Data Used in Solving Equation (25)

and Plotted in Figure 7

t	$\epsilon^{-\frac{Rt}{L}}$	$1 - \epsilon^{-\frac{Rt}{L}}$	$i_2(t) \times \frac{k}{R}$
$\frac{\pi}{8}\frac{L}{R}$	0.675	0.325	0.325
$\frac{\pi}{4}\frac{L}{R}$	0.456	0.544	0.544
$\frac{3\pi}{8}\frac{L}{R}$	0.307	0.693	0.693
$\frac{\pi}{2}\frac{L}{R}$	0.280	0.790	0.790
$\frac{5\pi}{8}\frac{L}{R}$	0.140	0.860	0.860
$\frac{3\pi}{4}\frac{L}{R}$	0.094	0.906	0.906
$\frac{7\pi}{8}\frac{L}{R}$	0.064	0.936	0.936
$\frac{\pi L}{R}$	0.043	0.957	0.957

TABLE II

Data Used in Plotting Equation (35)

t	$\epsilon^{-\frac{Rt}{L}}$	$0.571\,\epsilon^{-\frac{Rt}{L}}$	$1 - 0.571\,\epsilon^{-\frac{Rt}{L}}$
$0.084\,\frac{L}{R}$	0.919	0.524	0.476
$0.168\,\frac{L}{R}$	0.845	0.483	0.517
$0.252\,\frac{L}{R}$	0.777	0.444	0.556
$0.335\,\frac{L}{R}$	0.715	0.408	0.592

Data Used in Plotting Equation (38)

t	$\epsilon^{-\frac{Rt}{L}}$	$0.815\,\epsilon^{-\frac{Rt}{L}}$
$0.335\,\frac{L}{R}$	0.715	0.583
$0.419\,\frac{L}{R}$	0.657	0.536
$0.503\,\frac{L}{R}$	0.605	0.494
$0.587\,\frac{L}{R}$	0.556	0.454
$0.671\,\frac{L}{R}$	0.511	0.416

TABLE III

Values and Ratings of Components Shown on Schematic Diagram of Vertical Push-Pull Deflection Amplifier

C-1	0.05 mfd., 450 volts
C-2	0.05 mfd., 450 volts
L	Deflection Coil
P-1	1,000,000 ohms
P-2	1,000,000 ohms
P-3	250,000 ohms
P-4	1,000,000 ohms
R-1	300,000 ohms, 1 watt
R-2	4700 ohms, 1 watt
R-3	100,000 ohms, 1 watt
R-4	100,000 ohms, 1 watt
R-5	250,000 ohms, 1 watt
R-6	400 ohms, 1 watt
R-7	400 ohms, 1 watt
R-8	3000 ohms, 1 watt
R-9	3000 ohms, 1 watt
V-1	1/2 6SN7-GT
V-2	1/2 6SN7-GT
V-3	6V6
V-4	6V6

TABLE IV

Values and Ratings of Components Shown on Schematic Diagram of Horizontal Push-Pull Deflection Amplifier

C-1	0.05 mfd., 450 volts
C-2	0.05 mfd., 450 volts
L	Deflection Coil
R-1	300,000 ohms, 1 watt
R-2	4700 ohms, 1 watt
R-3	100,000 ohms, 1 watt
R-4	100,000 ohms, 1 watt
R-5	250,000 ohms, 1 watt
R-6	270 ohms, 1/2 watt
R-7	270 ohms, 1/2 watt
P-1	1,000,000 ohms
P-2	1,000,000 ohms
P-3	250,000 ohms
V-1	1/2 6SN7-GT
V-2	1/2 6SN7-GT
V-3	6L6
V-4	6L6

TABLE V

Data Taken with Circuit Shown in Figure 1, Appendix I, and Plotted in Figure 2, Appendix I, for Determining Parameters of the Deflection Coils

C	C'	f	$\frac{1}{f^2} \times 10^{-9}$
Vertical Coil:			
100 uuf	84 uuf	23.5 kc	1.81
200 uuf	184 uuf	20.8 kc	2.31
300 uuf	284 uuf	17.7 kc	3.19
400 uuf	384 uuf	15.8 kc	4.00
500 uuf	484 uuf	15.5 kc	4.16
Horizontal Coil:			
100 uuf	84 uuf	59.0 kc	0.287
200 uuf	184 uuf	41.9 kc	0.570
300 uuf	284 uuf	37.8 kc	0.700
400 uuf	384 uuf	34.1 kc	0.860
500 uuf	484 uuf	30.8 kc	1.052

APPENDIX III

DIAGRAMS

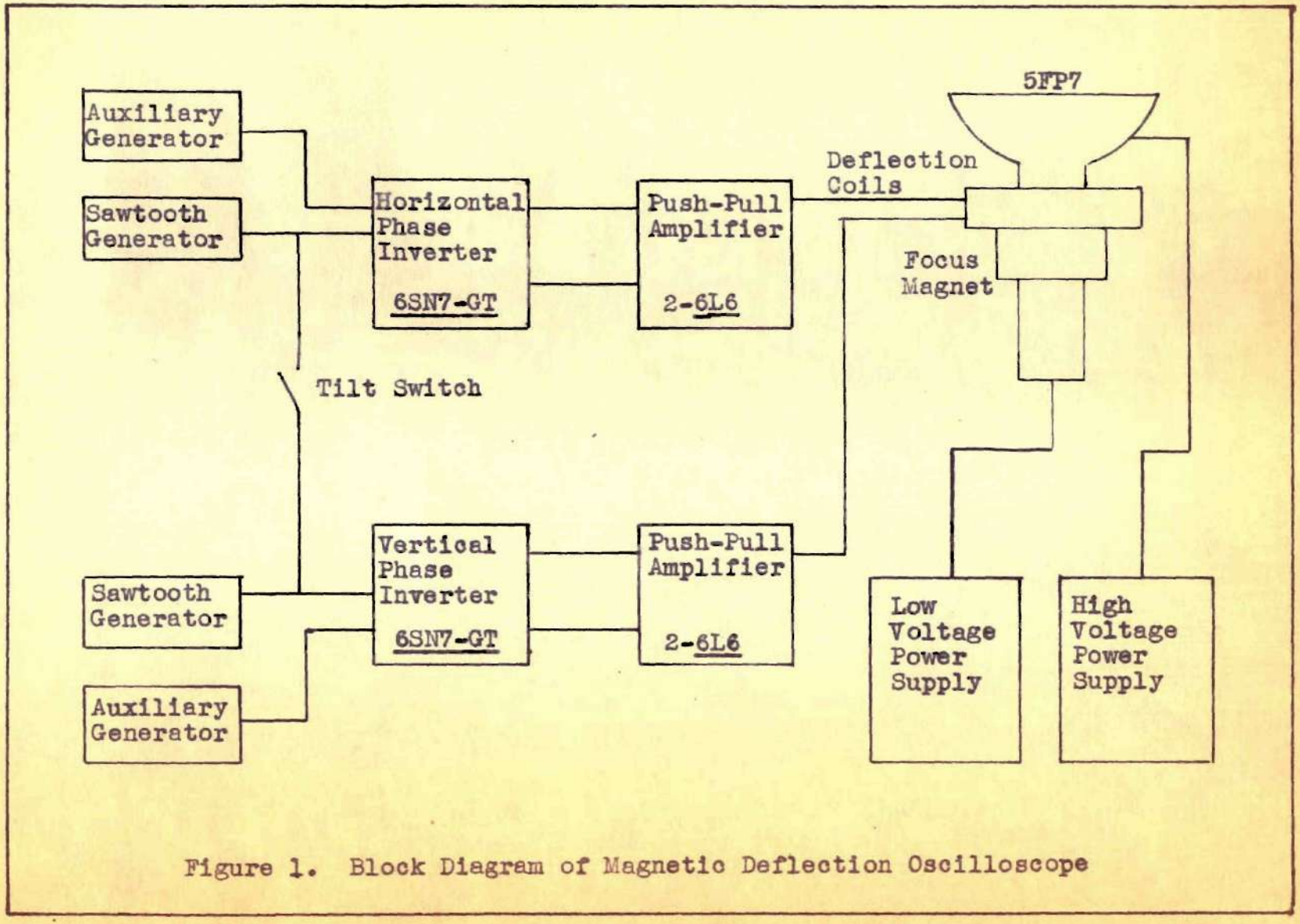

Figure 1. Block Diagram of Magnetic Deflection Oscilloscope

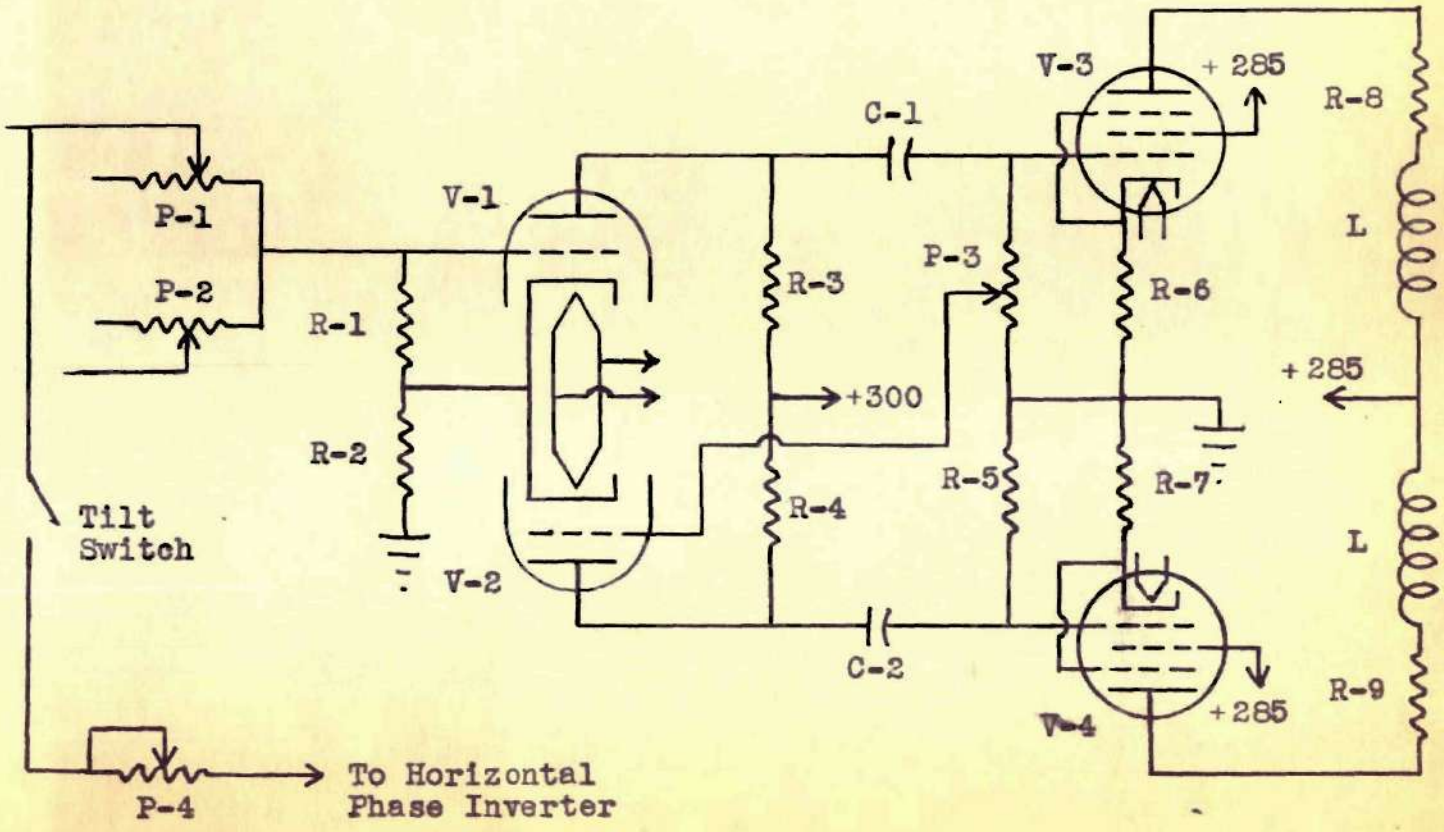

Figure 2. Vertical Push-Pull Deflection Amplifier

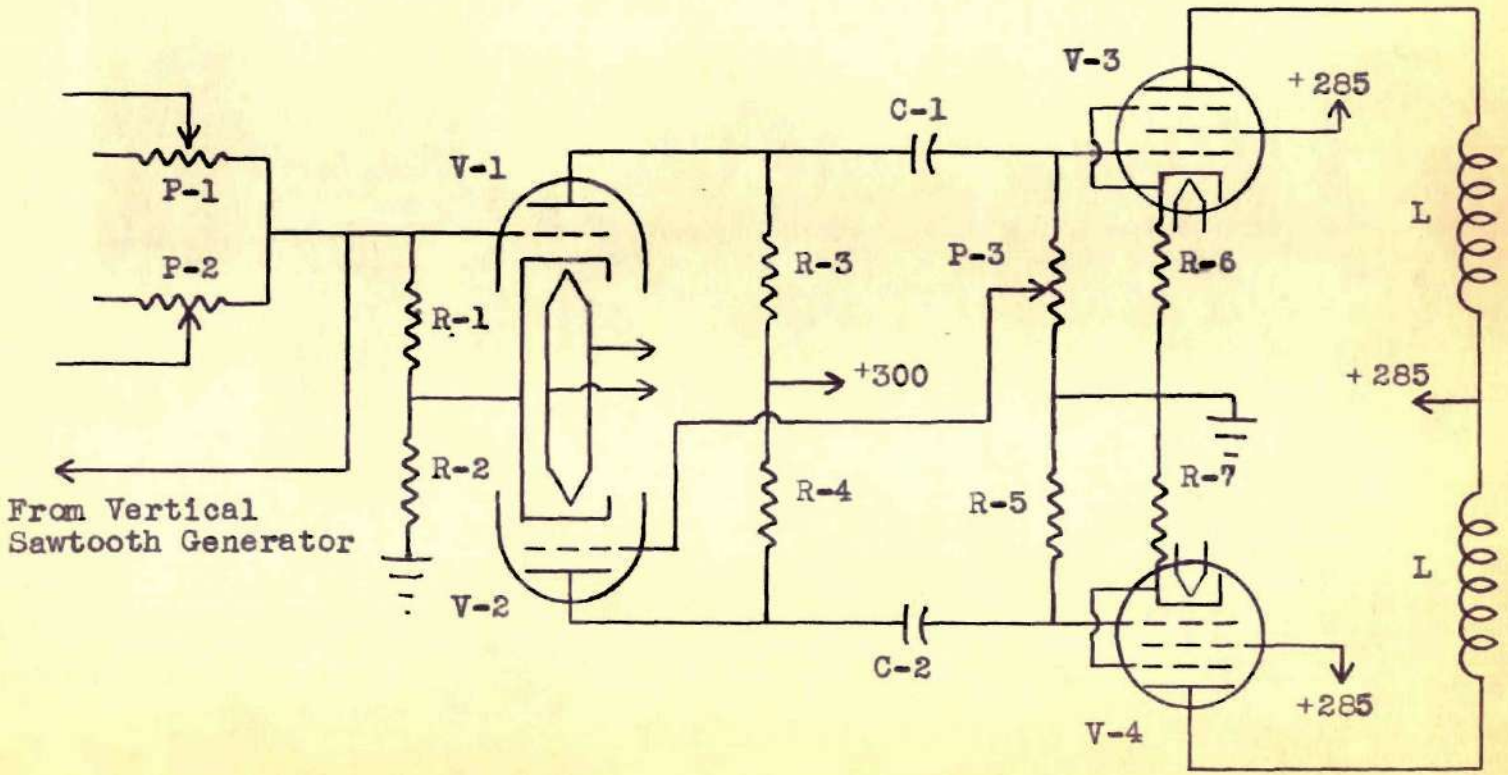

Figure 3. Horizontal Push-Pull Deflection Amplifier

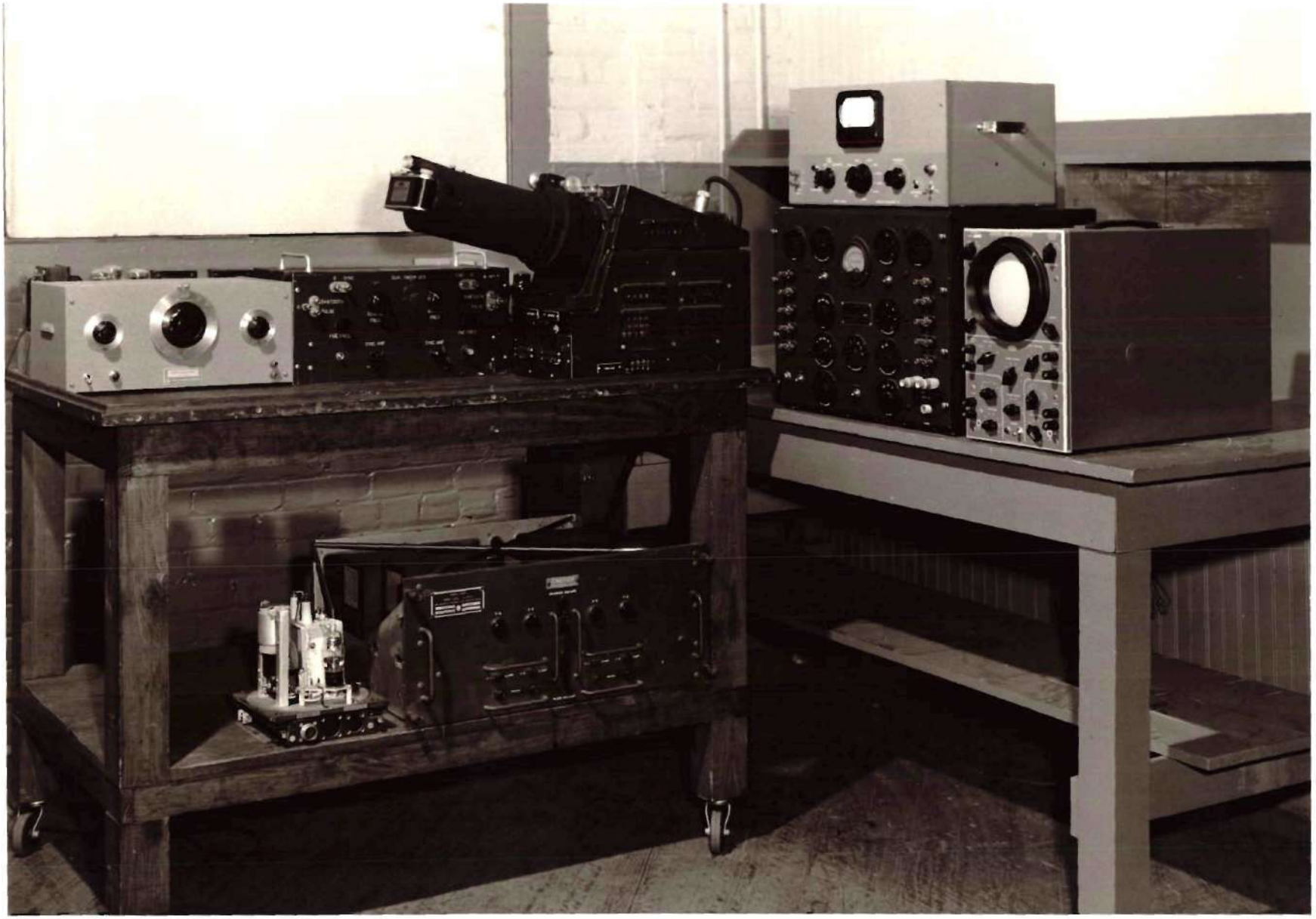

Figure 4 Magnetic Deflection Oscilloscope and Associated Laboratory Equipment.

APPENDIX IV

THREE-DIMENSIONAL PRESENTATIONS

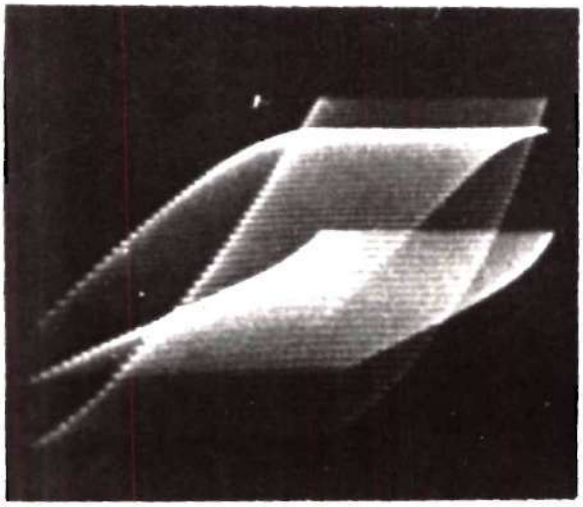

(a) V = 145 cps. sawtooth + 48 cps. sine wave.
H = 7.4 kc. sawtooth + 145 cps. sawtooth.

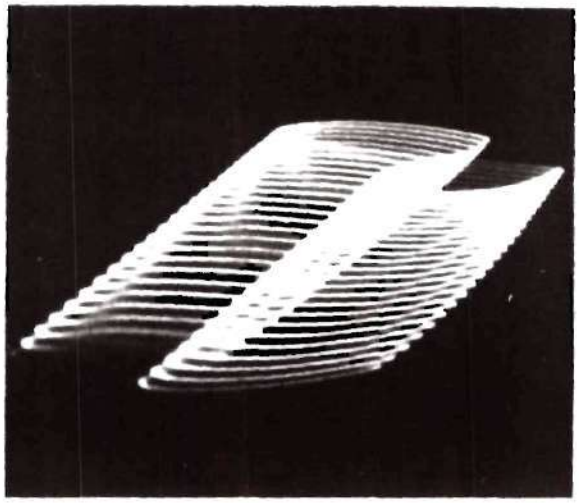

(b) V = 165 cps. sawtooth + 4600 cps. sine wave.
H = 8600 cps. sawtooth + 165 cps. sawtooth.

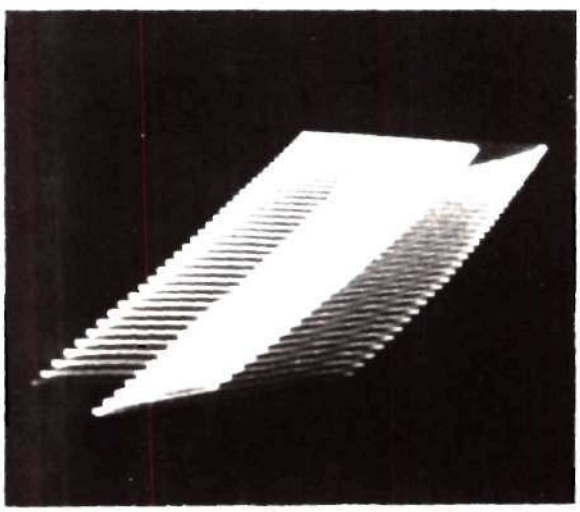

(c) V = 165 cps. sawtooth + 6.8 kc. sine wave.
H = 12.5 kc. sawtooth + 165 cps. sawtooth.

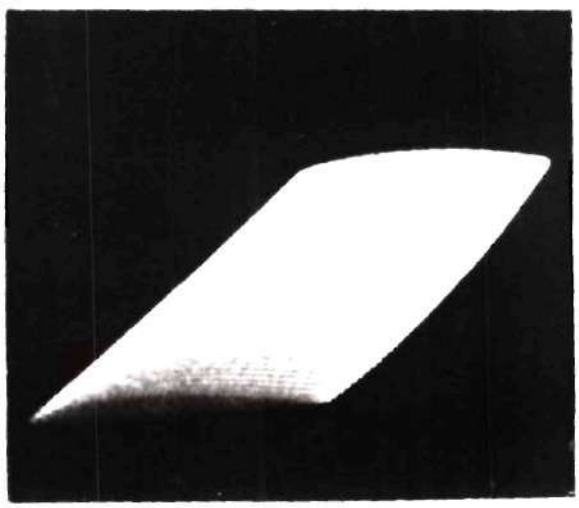

(d) V = 165 cps. sawtooth + 11.5 kc. sine wave.
H = 12.5 kc. sawtooth + 165 cps. sawtooth.

Figure 1. Three Dimensional Presentations

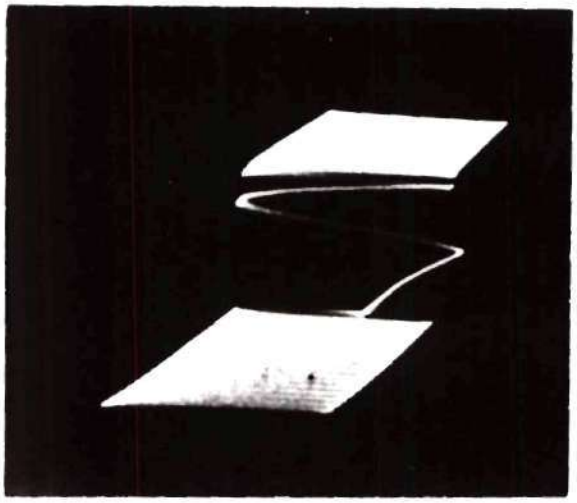

(a) V = 145 cps. sawtooth + 175 cps. square wave.
H = 7.3 kc. sawtooth + 145 cps. sawtooth.

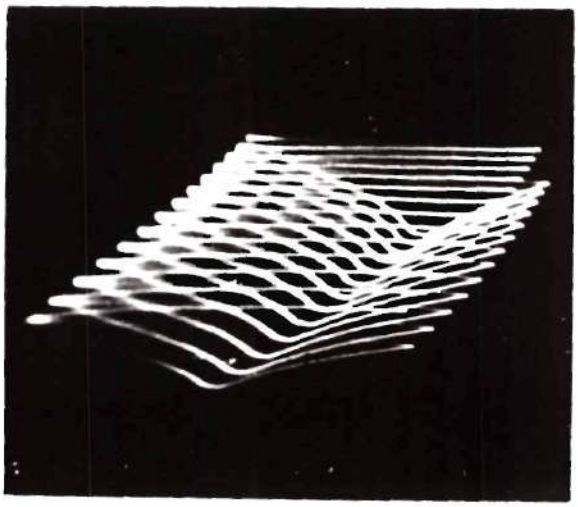

(b) V = 145 cps. sawtooth + 2 kc. square wave.
H = 7.8 kc. sawtooth + 145 cps. sawtooth.

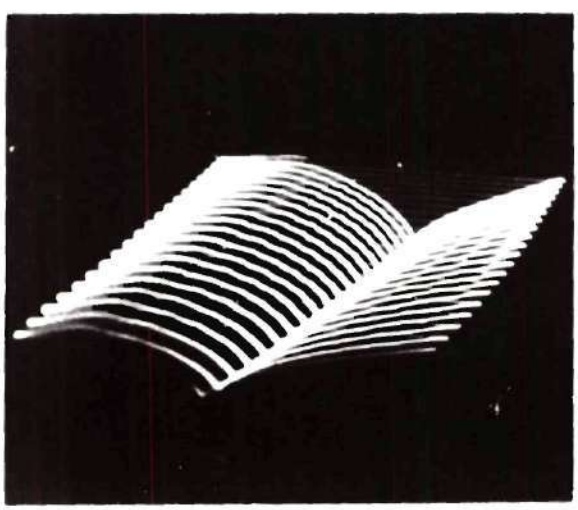

(c) V = 145 cps. sawtooth + 3 kc. square wave.
H = 7.8 kc. sawtooth + 145 cps. sawtooth.

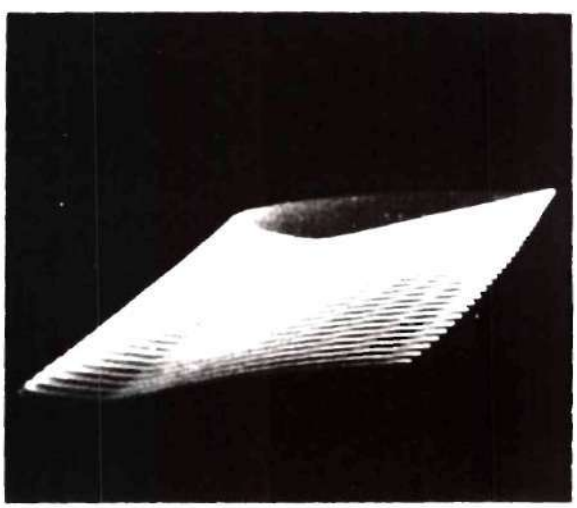

(d) V = 145 cps. sawtooth + 5 kc. square wave.
H = 7.8 kc. sawtooth + 145 cps. sawtooth.

Figure 2. Three Dimensional Presentations

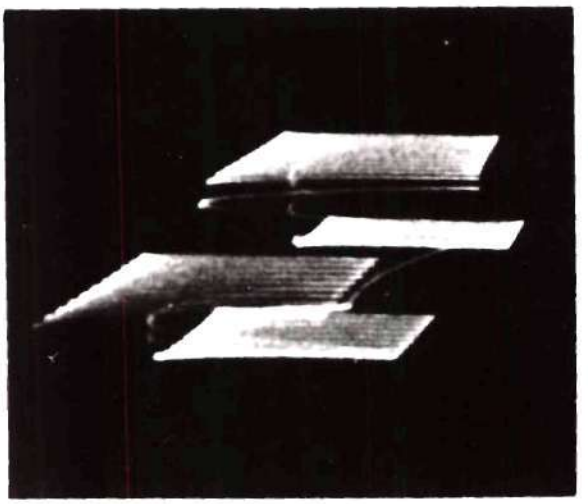

(a) V = 145 cps. sawtooth + 300 cps. square wave.
H = 7.8 kc. sawtooth + 145 cps. sawtooth.

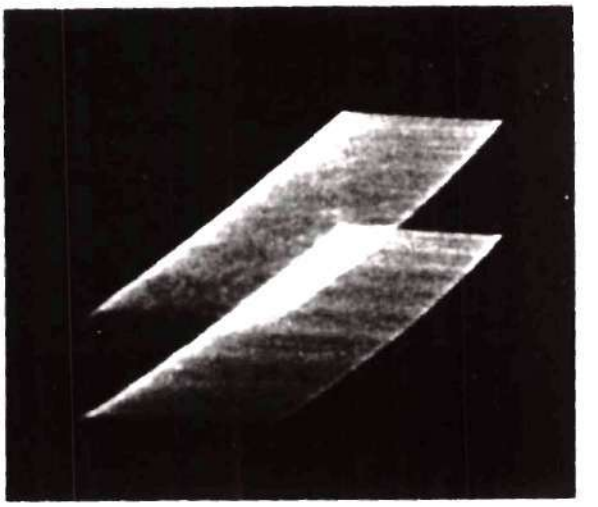

(b) V = 145 cps. sawtooth + 500 cps. square wave drifting.
H = 7.8 kc. sawtooth + 145 cps. sawtooth

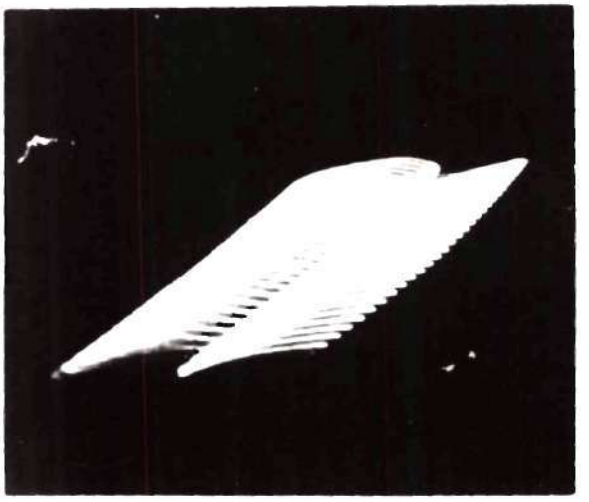

(c) V = 145 cps. sawtooth + 10 kc. square wave.
H = 7.8 kc. sawtooth + 145 cps. sawtooth.

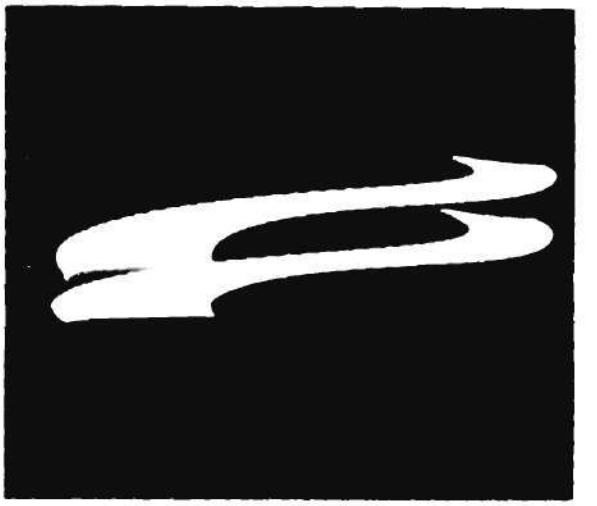

(d) V = 145 cps. sawtooth + 160 cps. square wave drifting.
H = 7.8 kc. sawtooth + 145 cps. sawtooth + 170 cps. sine wave.

Figure 3. Three Dimensional Presentations

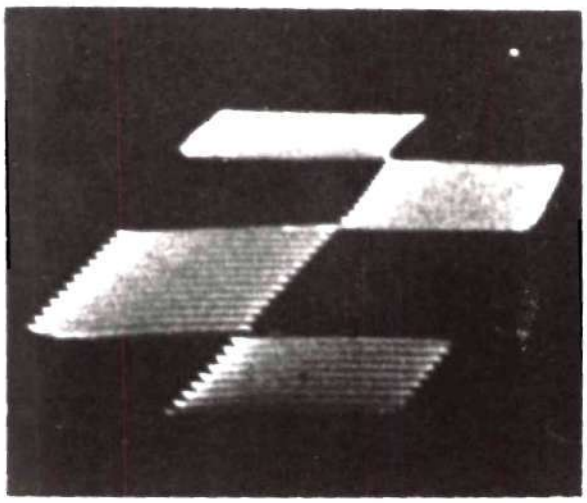

(a) V 145 cps. sawtooth.
H 8.6 kc. sawtooth +
145 cps. sawtooth +
335 cps. square wave.

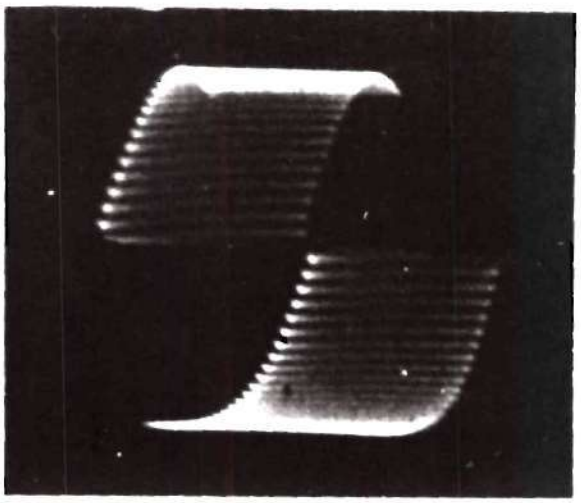

(b) V 145 cps. sawtooth +
180 cps. sine wave.
H 8.6 kc. sawtooth
145 cps. sawtooth
165 cps. square wave.

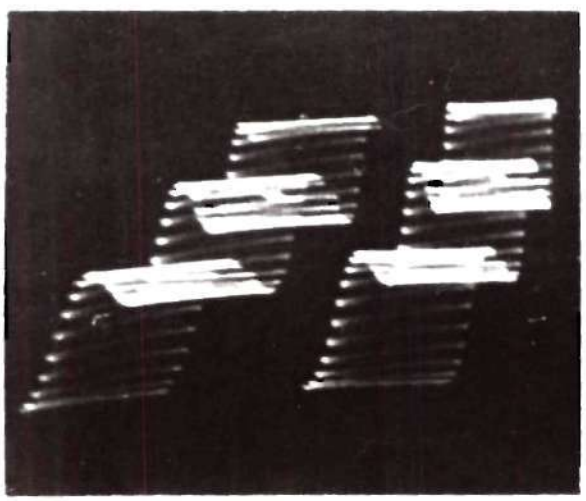

(c) V 145 cps. sawtooth +
560 cps. sine wave.
H 8.6 kc. sawtooth +
145 cps. sawtooth +
250 cps. square wave.

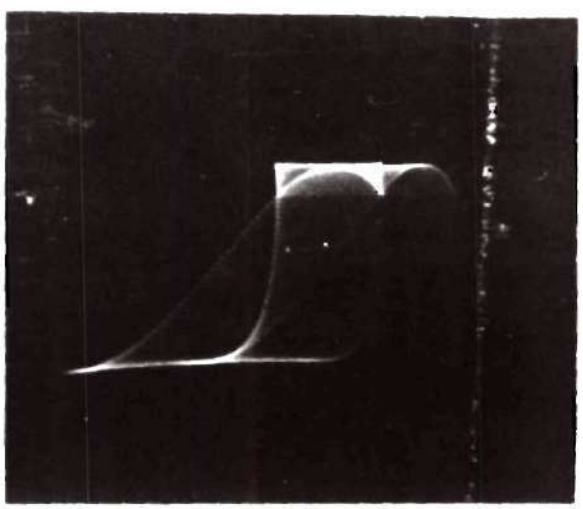

(d) V 145 cps. sawtooth +
180 cps. sine wave.
H 13 kc. sawtooth +
145 cps. sawtooth +
80 cps. sine wave.

Figure 4. Three Dimensional Presentations

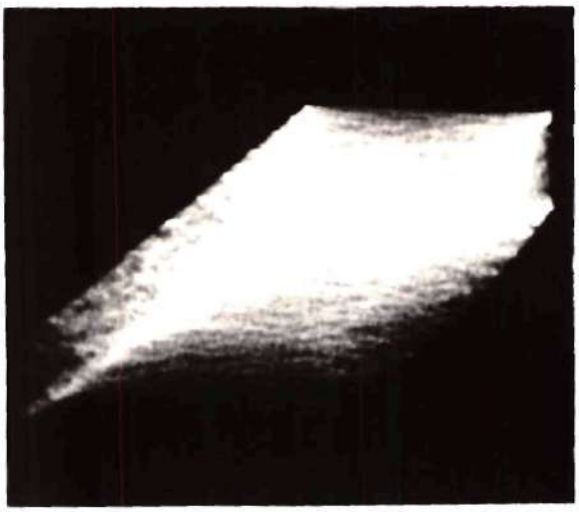

(a) V = 145 cps. sawtooth + 2.8 kc. sine wave drifting.
H = 6.4 kc. sawtooth + 145 cps. sawtooth.

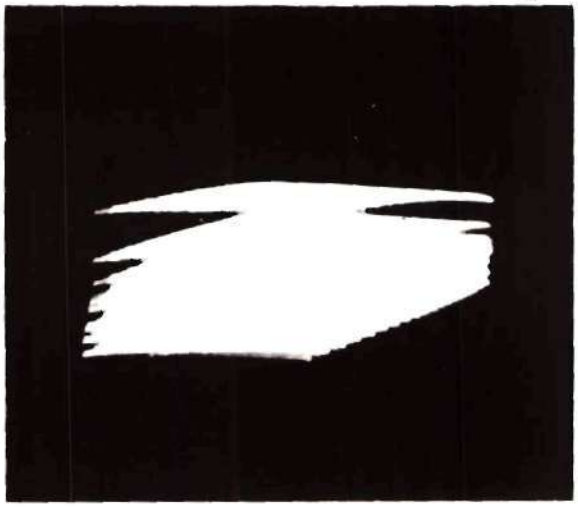

(b) V = 85 cps. sawtooth + 7 cps. sawtooth.
H = 2 kc. sawtooth + 85 cps. sawtooth.

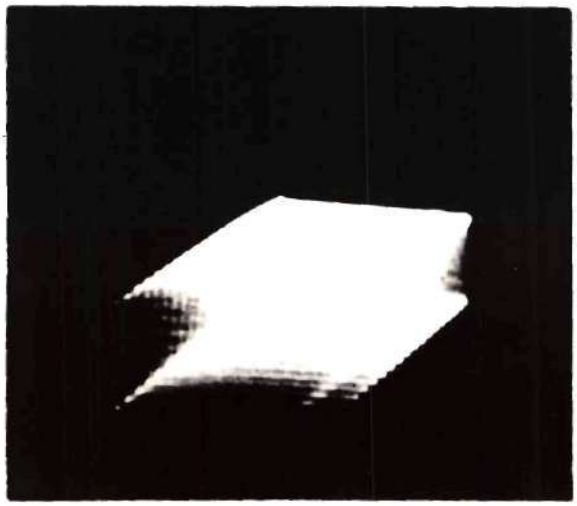

(c) V = 490 cps. sawtooth + 390 cps. sawtooth.
H = 10.5 kc. sawtooth + 490 cps. sawtooth + 2 kc. pulse to grid of CRT.

Figure 5. Three Dimensional Presentations

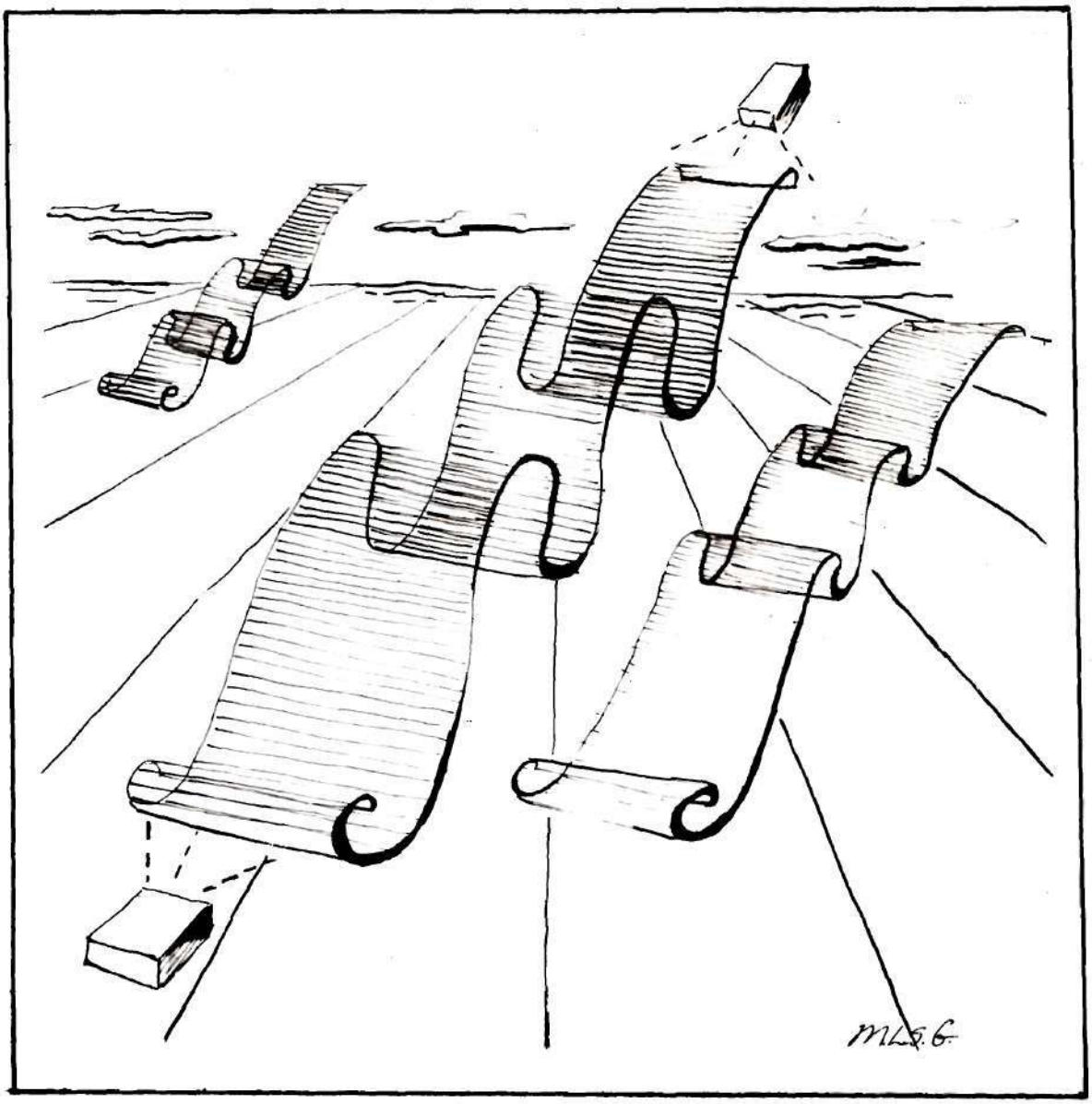
MLG.